

# eCP: Informative uncertainty quantification via Equivariantized Conformal Prediction with pre-trained models

Nikolaos Bousias<sup>1</sup>, Lars Lindemann<sup>2,3</sup>, and George Pappas<sup>1</sup>

<sup>1</sup>GRASP Lab, University of Pennsylvania

<sup>2</sup>Department of Computer Science, University of Southern California

<sup>3</sup>Automatic Control Laboratory, ETH Zürich

## Abstract

We study the effect of group symmetrization of pre-trained models on conformal prediction (CP), a post-hoc, distribution-free, finite-sample method of uncertainty quantification that offers formal coverage guarantees under the assumption of data exchangeability. Unfortunately, CP uncertainty regions can grow significantly in long horizon missions, rendering the statistical guarantees uninformative. To that end, we propose infusing CP with geometric information via group-averaging of the pretrained predictor to distribute the non-conformity mass across the orbits. Each sample now is treated as a representative of an orbit, thus uncertainty can be mitigated by other samples entangled to it via the orbit inducing elements of the symmetry group. Our approach provably yields contracted non-conformity scores in increasing convex order, implying improved exponential-tail bounds and sharper conformal prediction sets in expectation, especially at high confidence levels. We then propose an experimental design to test these theoretical claims in pedestrian trajectory prediction.

## 1 Introduction

Modern machine learning systems are increasingly deployed in settings where reliable uncertainty quantification is essential, such as robotics, autonomous navigation, and long-horizon forecasting. Conformal prediction (CP) has emerged as a principled and widely adopted framework for this purpose, providing finite-sample, distribution-free prediction sets with formal coverage guarantees under the mild assumption of data exchangeability [1, 2]. Crucially, CP is post-hoc and model-agnostic: it can be applied on top of any pretrained predictor without retraining or architectural modification. Split conformal prediction extends this framework to modern supervised learning settings by separating training and calibration data [3].

Despite these strengths [4], a well-known limitation of conformal prediction is efficiency. While coverage is guaranteed by design, the resulting prediction sets can become excessively large—particularly at high confidence levels or over long horizons—rendering the uncertainty estimates practically uninformative. This issue is especially pronounced in sequential decision-making and trajectory prediction tasks, where compounding uncertainty quickly leads to overly conservative prediction regions. Recent work has proposed adaptive, weighted, and conditional variants of CP to improve efficiency without sacrificing coverage [5–7].

At the same time, many real-world learning problems exhibit geometric or structural symmetries, such as translation, rotation, reflection, or time-shift invariance. These symmetries are often explicitly exploited during model training via data augmentation, equivariant architectures [8,9] or, more broadly, geometric deep learning approaches [10]. However, once a model is pretrained, such symmetry information is typically not leveraged during uncertainty quantification. Standard conformal prediction treats each sample in isolation, ignoring the fact that multiple transformed versions of the same input may be equivalent under a known symmetry group.

In this work, we show that explicitly incorporating group symmetries into conformal prediction—without retraining the model—can substantially reduce uncertainty while preserving coverage guarantees. We introduce Equivariantized Conformal Prediction (eCP), a simple and general post-hoc procedure that infuses

geometric information into CP by group-averaging the nonconformity score of a pretrained predictor. Rather than treating each data point as independent, eCP treats it as a representative of its entire group orbit, effectively redistributing nonconformity mass across symmetry-related samples.

## 1.1 Related work

Conformal prediction (CP) provides a general framework for constructing prediction sets with finite-sample coverage guarantees under exchangeability, independent of the underlying predictive model. CP was originally introduced in the algorithmic learning framework and has since been extended to regression, classification, and structured prediction problems [1–3]. Modern surveys provide a comprehensive overview of conformal methods and their applications in machine learning [4]. While validity is guaranteed by design, the efficiency of conformal prediction sets—measured by their size or tightness—depends critically on the choice of nonconformity score and the informativeness of the underlying predictor.

Several approaches aim to reduce the conservatism of CP sets by adapting the nonconformity score or calibration procedure. Examples include conformalized quantile regression [5], weighted conformal prediction under covariate shift [6], and adaptive conformal inference under distribution shift [7]. These methods improve efficiency but do not explicitly exploit known symmetry structure in the data, even when such structure is central to the learning problem.

Conformal prediction under geometric distribution shifts such as rotations or flips was studied in [11] by integrating canonicalization—learning to map inputs to a canonical pose—into the conformal pipeline to restore approximate exchangeability and maintain coverage under geometric shifts with primary goal being robustness: ensuring that conformal guarantees remain valid when test data differ geometrically from calibration data. Contrary to [11], eCP requires no additional learning and applies directly to any pretrained predictor via group averaging.

## 1.2 Safe Planning with Conformal Prediction

Uncertainty-aware motion planning in dynamic, human-populated environments is a central challenge in robotics and autonomous systems. In pedestrian-rich settings, planners must account for multi-modal, long-horizon uncertainty in human motion while providing formal safety guarantees. Several works have explored conformal prediction for sequential and multi-step forecasting problems relevant to safe planning. Sun and Yu [12] propose copula-based conformal prediction to model dependencies across time in multi-step time series prediction, producing calibrated uncertainty regions that better capture temporal correlations. While effective for forecasting, such approaches primarily focus on improving predictive calibration rather than planner-facing geometric structure. A complementary line of work emphasizes the *shape* and *usability* of conformal prediction regions for control and planning. Tumu *et al.* [13] introduce optimized convex shape templates for multi-modal conformal prediction regions, enabling compact, planner-friendly uncertainty sets that can be efficiently integrated into motion planning pipelines. Their approach highlights the importance of producing prediction regions that are not only statistically valid but also computationally practical for safety-critical systems. Conformal prediction has also been explicitly integrated into safe planning frameworks [14] in dynamic environments by treating conformal prediction regions as probabilistic safety envelopes around predicted agent trajectories. This framework provides formal safety guarantees under uncertainty and demonstrates the effectiveness of conformal sets in real-time planning scenarios. More recently, Sun *et al.* [15] combine conformal prediction with diffusion-based dynamics models to enable uncertainty-aware planning under complex, learned stochastic dynamics. Their method produces calibrated trajectory uncertainty sets that can be used to reason about safety constraints during planning.

### 1.2.1 Symmetries in Machine Learning

Geometric symmetries such as translation, rotation, reflection, and permutation play a central role in many learning tasks. Group equivariant neural networks encode symmetry directly into model architectures and have shown improved data efficiency and generalization [8,9,16,17]. More generally, geometric deep learning provides a unifying framework for learning on structured, non-Euclidean domains [10]. When architectural equivariance is unavailable or impractical, data augmentation [18] is often used as a heuristic alternative, though it provides no formal guarantees.

A closely related line of work studies predictive inference under group invariance assumptions. In particular, [19] develops a general framework for distribution-free predictive inference under arbitrary group symmetries [20, 21]. In contrast to these approaches, eCP operates within the classical split conformal setting and focuses on improving efficiency rather than generalizing the underlying inference model.

While symmetry-aware models are now well studied, comparatively less attention has been given to incorporating symmetry into post-hoc uncertainty quantification. In many practical pipelines, uncertainty estimates are constructed after training using pretrained models whose symmetry properties may be approximate or implicit rather than exact.

### 1.3 Why symmetrizing predictors enhances uncertainty quantification

Conformal prediction constructs uncertainty sets by calibrating a nonconformity score, which measures how atypical a candidate prediction is relative to past data. The efficiency of conformal prediction—i.e., the tightness of its prediction sets—is therefore governed not by the predictor alone, but by the distributional properties of these scores, particularly their tail behavior. In many learning problems, the input–output relationship exhibits known symmetries, such as invariance to rotations, translations, or time shifts. Standard conformal prediction, however, evaluates nonconformity at a single, arbitrary representative of the input, implicitly conditioning on a particular pose or coordinate frame. This can inject unnecessary variability into the nonconformity scores: two symmetry-equivalent inputs may produce noticeably different scores simply due to nuisance transformations, even though they carry the same semantic information.

Symmetrized nonconformity addresses this issue by explicitly aggregating nonconformity scores across the group orbit of the input. Rather than computing a score from one realization, we average the score over symmetry-related transformations. Intuitively, this treats each sample not as an isolated point, but as a representative of an entire equivalence class induced by the group action. This averaging has two key effects. First, it reduces variance by smoothing out fluctuations caused by arbitrary nuisance transformations. Second, it suppresses extreme values: large nonconformity scores that arise only for particular poses are diluted when averaged with more typical symmetry-related realizations. As a result, the symmetrized score distribution becomes more concentrated and exhibits lighter tails.

From a probabilistic perspective, symmetrization acts as a form of variance reduction without biasing coverage. Importantly, this does not require the underlying predictor to be exactly equivariant. Even approximate or emergent symmetry in the model’s behavior is sufficient for group averaging to contract the score distribution. Because conformal prediction sets are determined by high quantiles of the calibration scores, improved tail behavior directly translates into smaller prediction sets, with the most pronounced gains appearing at high confidence levels.

Symmetrized nonconformity leverages known symmetry structure to remove irrelevant variability from the calibration process. By redistributing nonconformity mass across symmetry orbits, it yields sharper and more informative conformal prediction sets while preserving the finite-sample guarantees of standard conformal prediction.

**Contributions:** This paper makes the following contributions:

1. We propose Equivariantized Conformal Prediction (eCP), a post-hoc method that incorporates group symmetries into conformal prediction via nonconformity score symmetrization, applicable to arbitrary pretrained models.
2. We establish that group-averaged nonconformity scores are contracted in increasing convex order, yielding improved tail behavior and sharper conformal prediction sets in expectation.
3. We demonstrate empirically that eCP significantly reduces uncertainty in long-horizon trajectory prediction tasks, particularly at high confidence levels, while maintaining formal coverage guarantees.

Overall, eCP provides a principled and practical mechanism for reducing conformal uncertainty by exploiting symmetry structure already present in the problem—bridging the gap between geometric inductive bias and post-hoc uncertainty quantification.

## 2 Preliminaries

### 2.1 Group Theory & Equivariant Functions

A group  $(G, \cdot)$  is a set  $G$  equipped with an operator  $\cdot : G \times G \rightarrow G$  that satisfies the properties of:

1. *Identity*:  $\exists e \in G$  such that  $e \cdot g = g \cdot e = e$
2. *Associativity*:  $\forall g, h, f \in G, g \cdot (h \cdot f) = (g \cdot h) \cdot f$
3. *Inverse*:  $\forall g \in G, \exists g^{-1}$  such that  $g^{-1} \cdot g = g \cdot g^{-1} = e$

Additional to its structure we can define the way that the group elements act on a space  $X$  via a group action:

**Definition 1.** A map  $\phi_g : X \rightarrow X$  is called an action of group element  $g \in G$  on  $X$  if for  $e$  identity element  $\phi_e(x) = x \forall x \in X$  and  $\phi_g \circ \phi_h = \phi_{g \cdot h} \forall g, h \in G$ .

When  $X$  is a vector space, the action of the group is defined through a linear group representation.

**Definition 2.** A linear group representation  $(V, \rho)$  of a group  $G$  is a map  $\rho : G \rightarrow GL(V)$  from group  $G$  to the general linear group  $GL(V)$ . The group action is then defined by the linear operator  $\phi_g[x] = \rho(g)x$  for all  $x \in V, g \in G$ .

Note here that a group action on a given space  $X$  allow us to group different elements of  $X$  in sets of orbits. More precisely given a group action  $\phi_*$  an orbit of a element  $x \in X$  is the set  $\mathcal{O}_x^{\phi_*} = \{\phi_g(x) | g \in G\}$ . In many application we require functions that respect the structure of a group acting on their domain and codomain. We refer to these functions as equivariant and we formally define them as follow:

**Definition 3.** Given a group  $G$  and corresponding group actions  $\phi_g : X \rightarrow X, \psi_g : X \rightarrow X$  for  $g \in G$  a function  $f : X \rightarrow Y$  is said to be  $(G, \phi_*, \psi_*)$ -equivariant if and only if  $\psi_g(f(x)) = f(\phi_g(x)) \forall x \in X, g \in G$ .

A spacial case of equivariance is  $G$ -invariance occuring if  $\psi_* := id$  and the function  $f$  is constant over group orbits of  $X$ , i.e.  $f \circ \phi_* \equiv f, \forall * \in G$ .

### 2.2 Conformal Prediction

Conformal prediction [1] is a framework for constructing predictive sets with finite-sample, distribution-free guarantees under minimal statistical assumptions. It provides a way to quantify uncertainty in machine learning predictions without relying on strong parametric assumptions about the data-generating process. The foundational assumption behind CP is exchangeability, which generalizes the i.i.d. assumption. A sequence of random variables  $Z_{1:n} = (Z_1, \dots, Z_n), Z_i = (X_i, Y_i)$  is *exchangeable* if

$$P(Z_1, \dots, Z_n) = P(Z_{\pi(1)}, \dots, Z_{\pi(n)})$$

for any permutation  $\pi \in \mathbb{S}_n$ , i.e. if its joint distribution is invariant to sample ordering. Under exchangeability, the ordering of data points carries no information, and this property enables the construction of valid p-values for candidate predictions, ensuring that calibration statistics computed on past data are valid for future predictions. This principle is what allows CP to maintain coverage guarantees even when the underlying model is misspecified or highly complex. We consider the setting of split conformal prediction, wherein a hold-out calibration set  $\mathcal{D}_{\text{cal}} = \{(x_i, y_i)\}_{i=1:n_c}$  and a test set  $\mathcal{D}_{\text{test}} = \{(x_i, y_i)\}_{i=1:n_t}$  are sampled under exchangeability for some fixed distribution [22]. Given a pretrained prediction model  $f_\theta$  and a non-conformity score function  $s : \mathcal{X} \times \mathcal{Y} \rightarrow \mathbb{R}$  measuring how atypical a sample is by encoding the disparity between prediction and label, we compute calibration scores  $s_i = s(f_\theta(x_i), y_i)$  on held-out  $\mathcal{D}_{\text{cal}}$ . The choice of nonconformity function strongly influences the efficiency/tightness of prediction sets but not their validity. For a new sample  $(x_{n_c+1}, y_{n_c+1})$ , define the prediction set

$$C_{1-\alpha}(x_{n_c+1}) = \{y \in \mathcal{Y} : s(f_\theta(x_{n_c+1}), y) \leq q_{1-\alpha}\},$$

where  $q_{1-\alpha}$  is the  $(1 - \alpha)$ -quantile of the empirical calibration non-conformity distribution  $S = \{s_{1:n_c}\}$  for tolerated miscoverage rate  $\alpha \in (0, 1)$ . Then, with high probability a valid coverage guarantee on inclusion of the true label  $y_{n_c+1}$  stands

$$P(y_{n_c+1} \in C_{1-\alpha}(x_{n_c+1})) \geq 1 - \alpha,$$

under exchangeability [3,5]. While validity is unconditional, efficiency — the expected size or tightness of the prediction set — depends on the informativeness of the model and the nonconformity function. In practice, a well-calibrated and expressive base model yields smaller, more informative sets.

### 3 Symmetries-infused Conformal Prediction

Let  $(\mathcal{X}, \mathcal{Y})$  be measurable spaces and  $G$  a (finite or compact) group acting measurably on  $\mathcal{X}$  and  $\mathcal{Y}$ . Let  $F \subset \mathcal{M}_b(\mathcal{X})$  be the set of bounded measurable functions  $f : \mathcal{X} \rightarrow \mathcal{Y}$  and define its subset of  $G$ -equivariant functions  $F_G := \{f \in F : f \circ \phi_g = \psi_g \circ f, \forall g \in G\}$ . A probability measure  $\mu \in \mathcal{P}(\mathcal{Z} = \mathcal{X} \times \mathcal{Y})$  is  $G$ -invariant if, for  $\tau_g := (\phi_g, \psi_g)$ ,  $\mu = \mu \circ \tau_g, \forall g \in G$ .

**Definition 4** (Group-invariant distribution). *Let  $Z = (X, Y)$  be a random variable with a probability distribution  $P$  on a sample space  $\mathcal{Z} = \mathcal{X} \times \mathcal{Y}$ . The distribution  $P$  is group invariant if  $P(\tau_g(A)) = P(A)$  for all  $g \in G$  and any measurable subset  $A \subseteq \mathcal{Z}$ .*

This is equivalent to saying that the joint probability measure is  $G$ -invariant and  $(X, Y) \stackrel{d}{=} (\phi_g(X), \psi_g(Y))$ . These structures generalize permutation invariance, i.e. exchangeability, to more general geometric or combinatorial symmetries.

**Definition 5** ( $G^{n+1}$ -Exchangeability). *A random sequence  $(Z_1, \dots, Z_{n+1})$  is  $G^{n+1}$ -exchangeable if*

$$(Z_1, \dots, Z_{n+1}) \stackrel{d}{=} (\tau_{g_1}(Z_1), \dots, \tau_{g_{n+1}}(Z_{n+1})) \quad \forall g_1, \dots, g_{n+1} \in G.$$

The  $G^{n+1}$ -exchangeability generalizes the exchangeability requirement of CP from just the permutation group  $S_{n+1}$ , to include the geometric transformations of samples by  $G^{n+1}$ , implying that the joint distribution is  $G^{n+1}$ -invariant.

**Assumption 1.** *The nonconformity score function  $s : F_G(\mathcal{X}) \times \mathcal{Y} \rightarrow \mathbb{R}$  is  $G$ -invariant in the sense that  $s(\psi_g(y_i), \psi_g(y_j)) = s(y_i, y_j), \forall g \in G$ .*

**Definition 6** (Symmetrization Operator). *For some  $G$ -invariant non-conformity score  $s : F_G(\mathcal{X}) \times \mathcal{Y} \rightarrow \mathbb{R}_{\geq 0}$ , define the score symmetrization operator  $\Pi : (F \times \mathcal{X}) \times \mathcal{Y} \rightarrow \mathbb{R}_{\geq 0}$  as:*

$$\Pi_G[s; f](x, y) := \int_G s(f(\phi_{g^{-1}}(x)), \psi_{g^{-1}}(y)) d\mu_G(g) = \mathbb{E}_{\mu_G} [s(f(\phi_{g^{-1}}(x)), \psi_{g^{-1}}(y))] \quad (1)$$

where  $\mu_G$  is the unique, left-invariant Haar probability measure on the compact Hausdorff topological group  $G$ , with  $\mu_G(G) = 1$ .

**Lemma 1** (Invariance and projection of  $\Pi_G$ ). *Under Assumption 1, the symmetrization operator  $\Pi$  is a  $G$ -invariant projection in the sense that*

$$\Pi_G[s; f](\phi_h(x), \psi_h(y)) = \Pi_G[s; f](x, y) \quad \forall h \in G, (x, y) \in \mathcal{X} \times \mathcal{Y}.$$

Moreover, if  $f \in F_G$  then  $\Pi_G[s; f](x, y) = s(f(x), y)$  for all  $(x, y)$  (idempotence on  $G$ -equivariant models).

*Proof.* By Definition 6 and left-invariance of the Haar probability measure  $\mu_G$ ,

$$\begin{aligned} \Pi_G[s; f](\phi_h(x), \psi_h(y)) &= \int_G s(f(\phi_{g^{-1}}\phi_h(x)), \psi_{g^{-1}}\psi_h(y)) d\mu_G(g) \\ &\stackrel{g' = h^{-1}g}{=} \int_{h \cdot G} s(f(\phi_{g'^{-1}}(x)), \psi_{g'^{-1}}(y)) d\mu_G(hg') \\ &= \int_G s(f(\phi_{g'^{-1}}(x)), \psi_{g'^{-1}}(y)) d\mu_G(g') = \Pi_G[s; f](x, y), \end{aligned}$$

where we used  $d\mu_G(g) = d\mu_G(g')$  and the group homomorphism property of the actions. If  $f \in F_G$ , then  $f \circ \phi_{g^{-1}} = \psi_{g^{-1}} \circ f$ , hence by  $G$ -invariance of  $s$  in Assumption 1,  $s(f(\phi_{g^{-1}}(x)), \psi_{g^{-1}}(y)) = s(\psi_{g^{-1}}f(x), \psi_{g^{-1}}(y)) = s(f(x), y)$ , so

$$\Pi_G[s; f](x, y) = \int_G s(f(x), y) d\mu_G(g) = s(f(x), y).$$

□

**Lemma 2.** *It stands that  $\Pi_G[s; f](x, y) = \mathbb{E}_{(\mathcal{X} \times \mathcal{Y}) \sim P}[s(f(X), Y) | (X, Y) \in \mathcal{O}_{(x, y)}^{(\phi, \psi)}]$ .*

*Proof.* Let  $(X, Y) \in \mathcal{O}_{(x, y)}^{(\phi, \psi)}$ . For some element  $g \in G$  it stands that

$$\begin{aligned} \mathbb{E}_{(\mathcal{X} \times \mathcal{Y}) \sim P}[s(f(X), Y) | (X, Y) \in \mathcal{O}_{(x, y)}^{(\phi, \psi)}] &= \int_{\mathcal{O}_{(x, y)}^{(\phi, \psi)}} s(f(X), Y) d\mu(X, Y) \\ &= \int_{\mathcal{X}, \mathcal{Y}} s(f(\phi_{g^{-1}}(X)), \psi_{g^{-1}}(Y)) \mathbf{1}\{(\phi_{g^{-1}}(X), \psi_{g^{-1}}(Y)) \in \mathcal{O}_{(x, y)}^{(\phi, \psi)}\} d\mu(X, Y) \\ &= \int_{\mathcal{X}, \mathcal{Y}} s(f(\phi_{g^{-1}}(X)), \psi_{g^{-1}}(Y)) \mathbf{1}\{(X, Y) \in \mathcal{O}_{(x, y)}^{(\phi, \psi)}\} d\mu(X, Y) \end{aligned}$$

By construction of the orbit,  $\exists g^* \in G$  s.t.  $x = \phi_{g^*}X$ . Taking expectations over the group yields:

$$\begin{aligned} \int_{\mathcal{O}_{(x, y)}^{(\phi, \psi)}} s(f(X), Y) d\mu(X, Y) &= \int_G \int_{\mathcal{X}, \mathcal{Y}} s(f(\phi_{g^{-1}}(X)), \psi_{g^{-1}}(Y)) \mathbf{1}\{(X, Y) \in \mathcal{O}_{(x, y)}^{(\phi, \psi)}\} d\mu(X, Y) d\mu_G(g) \\ &= \int_G \int_{\mathcal{X}, \mathcal{Y}} s(f(\phi_{g^{-1}g^{*-1}}(x)), \psi_{g^{-1}g^{*-1}}(y)) \mathbf{1}\{(X, Y) \in \mathcal{O}_{(x, y)}^{(\phi, \psi)}\} d\mu(X, Y) d\mu_G(g) \\ &\stackrel{Fubini}{=} \int_{\mathcal{X}, \mathcal{Y}} \int_G s(f(\phi_{g^{-1}g^{*-1}}(x)), \psi_{g^{-1}g^{*-1}}(y)) d\mu_G(g) \mathbf{1}\{(X, Y) \in \mathcal{O}_{(x, y)}^{(\phi, \psi)}\} d\mu(X, Y) \\ &\stackrel{\text{Lemma 1}}{=} \int_{\mathcal{X}, \mathcal{Y}} \int_G s(f(\phi_{g^{-1}}(x)), \psi_{g^{-1}}(y)) d\mu_G(g) \mathbf{1}\{(X, Y) \in \mathcal{O}_{(x, y)}^{(\phi, \psi)}\} d\mu(X, Y) \\ &= \int_{\mathcal{O}_{(x, y)}^{(\phi, \psi)}} \Pi_G[s; f](x, y) d\mu(X, Y) = \Pi_G[s; f](x, y) \end{aligned}$$

□

**Corollary 1.** *From the law of total probability, the mean of the score symmetrization operator is the same as that of the score function itself, i.e.  $\mathbb{E}_{\mathcal{X} \times \mathcal{Y} \sim P}[\Pi_G[s; f](X, Y)] = \mathbb{E}_{\mathcal{X} \times \mathcal{Y} \sim P}[s(f(X), Y)]$ .*

**Theorem 1** (Finite-Sample Validity of Equivariantized Split Conformal Prediction). *Consider  $\mathcal{D}_{\text{train}}$  training set and  $\mathcal{D}_{\text{cal}} = \{(X_i, Y_i)\}_{i=1:n_c}$  calibration set, both drawn from a  $G$ -invariant distribution  $P$  on  $\mathcal{X} \times \mathcal{Y}$  (hence the calibration samples and the test sample  $(X_{n_c+1}, Y_{n_c+1})$  are  $G^{n_c+1} \times \mathbb{S}_{n_c+1}$ -exchangeable), and let Assumption 1 stand. Define group invariant calibration scores  $\tilde{S}_i = \Pi[s; f](X_i, Y_i)$  for  $(X_i, Y_i) \in \mathcal{D}_{\text{cal}}$  and, for any test sample  $x_{n_c+1} \in \mathcal{X}$  and candidate label  $y \in \mathcal{Y}$ , define the test score  $\tilde{S}_{n_c+1}(y) = \Pi[s; f](X_{n_c+1}, y)$ . Let  $\tilde{S}_{(1)} \leq \dots \leq \tilde{S}_{(m)}$  denote the ordered calibration scores and, for some miscoverage rate  $\alpha \in (0, 1)$ , let*

$$k = \lceil (m+1)(1-\alpha) \rceil, \quad q = \tilde{S}_{(k)}.$$

*Then, for equivariant split conformal prediction set  $C_{1-\alpha}^{(G)}(X_{n_c+1}) = \{y \in \mathcal{Y} : \tilde{S}_{n_c+1}(y) \leq q\}$  it stands that*

$$P(Y_{n_c+1} \in C_{1-\alpha}^{(G)}(X_{n_c+1}) | \mathcal{D}_{\text{train}}) \geq 1 - \alpha$$

*Proof.* By Assumption 1,  $\Pi[s; f]$  is the same measurable map applied to every index and is  $G$ -invariant:

$$\Pi[s; f](g \cdot x, g \cdot y) = \Pi[s; f](x, y) \quad \forall g \in G.$$

Because the calibration points and test point are drawn from a  $G$ -invariant law and are permutation-exchangeable across indices (as stated in the theorem), the  $(m+1)$ -tuple

$$((X_1, Y_1), \dots, (X_m, Y_m), (X_{m+1}, Y_{m+1}))$$

is exchangeable under index permutations, conditional on  $\mathcal{D}_{\text{train}}$ . Applying the same coordinatewise function  $(x, y) \mapsto \Pi[s; f](x, y)$  preserves exchangeability. Therefore the *score vector*

$$(\tilde{S}_1, \dots, \tilde{S}_m, \tilde{S}_{m+1}(Y_{m+1})) \quad \text{with} \quad \tilde{S}_i := \Pi[s; f](X_i, Y_i), \quad \tilde{S}_{m+1}(y) := \Pi[s; f](X_{m+1}, y)$$

is exchangeable conditional on  $\mathcal{D}_{\text{train}}$ .

Let  $\tilde{S}_{(1)} \leq \dots \leq \tilde{S}_{(m)}$  denote the ordered calibration scores and set  $k = \lceil (m+1)(1-\alpha) \rceil$ ,  $q = \tilde{S}_{(k)}$ . Define the rank

$$R := |\{i \in \{1, \dots, m+1\} : \tilde{S}_i \geq \tilde{S}_{m+1}(Y_{m+1})\}|.$$

By exchangeability of the score vector, conditional on  $\mathcal{D}_{\text{train}}$  the rank  $R$  is uniform on  $\{1, \dots, m+1\}$  after standard randomized tie-breaking; without randomization, it is stochastically no smaller than the uniform law, yielding a conservative inequality.

By construction,  $\tilde{S}_{m+1}(Y_{m+1}) \leq q$  if and only if  $R \leq k$ . Hence,

$$P(\tilde{S}_{m+1}(Y_{m+1}) \leq q \mid \mathcal{D}_{\text{train}}) = \Pr(R \leq k \mid \mathcal{D}_{\text{train}}) \geq \frac{k}{m+1} \geq 1-\alpha.$$

But  $\{\tilde{S}_{m+1}(Y_{m+1}) \leq q\}$  is exactly the event  $\{Y_{m+1} \in C_{1-\alpha}^{(G)}(X_{m+1})\}$ , which proves

$$P(Y_{m+1} \in C_{1-\alpha}^{(G)}(X_{m+1}) \mid \mathcal{D}_{\text{train}}) \geq 1-\alpha.$$

If ties occur with probability zero (e.g., when  $\Pi[s; f](X, Y)$  has a continuous distribution), the non-randomized rule attains coverage  $k/(m+1)$ , which differs from  $1-\alpha$  by at most  $1/(m+1)$ ; with randomized tie-breaking it equals  $1-\alpha$  exactly. Moreover,  $G$ -invariance of  $\Pi[s; f]$  implies the natural equivariance of the predictor:  $\tilde{S}_{m+1}(y) \leq q \iff \tilde{S}_{m+1}(\psi_g(y)) \leq q, \forall g \in G$ , so  $C_{1-\alpha}^{(G)}(\phi_g(x)) = \psi_g \circ C_{1-\alpha}^{(G)}(x), \forall g \in G$ .  $\square$

**Corollary 2** (Variance reduction under symmetrized non-conformity scores). *Let  $P$  be a  $G$ -invariant probability measure on  $\mathcal{X} \times \mathcal{Y}$ , let  $Z := s(f(X), Y) \in L^2(P)$ , and let*

$$\Pi_G[s; f](X, Y) = \int_G s(f(\phi_{g^{-1}}(X)), \psi_{g^{-1}}(Y)) d\mu_G(g) = \mathbb{E}[Z \mid \sigma(G)],$$

where  $\mu_G$  is the Haar probability measure on the compact group  $G$  and  $\sigma(G)$  is the  $\sigma$ -algebra of  $G$ -invariant events. Then, from the total variance law:

$$\text{Var}(Z) = \text{Var}(\mathbb{E}[Z \mid \sigma(G)]) + \mathbb{E}[\text{Var}(Z \mid \sigma(G))] = \text{Var}(\Pi_G[s; f]) + \mathbb{E}[\text{Var}(Z \mid \sigma(G))] \quad (2)$$

and hence

$$\text{Var}(Z) - \text{Var}(\Pi_G[s; f]) = \mathbb{E}[\text{Var}(Z \mid \sigma(G))] \geq 0, \quad (3)$$

with equality iff  $Z$  is  $G$ -invariant almost surely.

Moreover, writing  $Z_g := s(f(\phi_{g^{-1}}(X)), \psi_{g^{-1}}(Y))$ , we have the orbit-averaging identities

$$\begin{aligned} \text{Var}(Z) - \text{Var}(\Pi_G[s; f]) &= \mathbb{E}[(Z - \Pi_G[s; f])^2] = \frac{1}{2} \mathbb{E} \left[ \int_G (Z - Z_g)^2 d\mu_G(g) \right] \\ &= \frac{1}{2} \mathbb{E} \left[ \iint_{G \times G} (Z_g - Z_h)^2 d\mu_G(g) d\mu_G(h) \right] \end{aligned} \quad (4)$$

If  $G$  is finite, with  $|G| < \infty$  and uniform counting measure, (4) becomes

$$\text{Var}(Z) - \text{Var}(\Pi_G[s; f]) = \frac{1}{2|G|} \mathbb{E} \left[ \sum_{g \in G} (Z - Z_g)^2 \right] = \frac{1}{2|G|^2} \mathbb{E} \left[ \sum_{g, h \in G} (Z_g - Z_h)^2 \right]. \quad (5)$$

*Proof.* We first recall that  $\Pi_G[s; f] = \mathbb{E}[Z \mid \sigma(G)]$  (Lemma 2 identifying  $\Pi_G$  with a conditional expectation onto  $G$ -orbits). The law of total variance yields (2) directly, and (3) follows by nonnegativity of conditional variance. Equality in (3) holds iff  $\text{Var}(Z \mid \sigma(G)) = 0$  a.s., i.e. iff  $Z$  is  $\sigma(G)$ -measurable, equivalently  $G$ -invariant almost surely (variance is eliminated within orbit for invariant scoring).

For the orbit identities, note first that

$$\mathbb{E}[(Z - \Pi_G[s; f])^2] = \mathbb{E}[Z^2] - 2\mathbb{E}[Z \Pi_G[s; f]] + \mathbb{E}[(\Pi_G[s; f])^2] = \mathbb{E}[Z^2] - \mathbb{E}[(\Pi_G[s; f])^2],$$

since  $\mathbb{E}[Z \Pi_G[s; f]] = \mathbb{E}[\mathbb{E}[Z \mid \sigma(G)] \Pi_G[s; f]] = \mathbb{E}[(\Pi_G[s; f])^2]$ .

Now introduce  $Z_g := s(f(\phi_{g^{-1}}(X)), \psi_{g^{-1}}(Y))$  and observe

$$\Pi_G[s; f] = \int_G Z_g d\mu_G(g), \quad \mathbb{E}[(\Pi_G[s; f])^2] = \mathbb{E}\left[\iint Z_g Z_h d\mu_G(g) d\mu_G(h)\right].$$

By  $G$ -invariance of  $P$  and Fubini,

$$\mathbb{E}[Z^2] = \mathbb{E}\left[\int_G Z_g^2 d\mu_G(g)\right] \tag{6}$$

Combining,  $\mathbb{E}[(Z - \Pi_G[s; f])^2] = \mathbb{E}\left[\int_G Z_g^2 d\mu_G(g)\right] - \mathbb{E}\left[\iint Z_g Z_h d\mu_G(g) d\mu_G(h)\right]$ . Symmetrizing the right-hand side gives

$$\mathbb{E}[(Z - \Pi_G[s; f])^2] = \frac{1}{2} \mathbb{E}\left[\iint (Z_g - Z_h)^2 d\mu_G(g) d\mu_G(h)\right],$$

which is the last equality in (4). Averaging one of the integrals out yields

$$\mathbb{E}[(Z - \Pi_G[s; f])^2] = \frac{1}{2} \mathbb{E}\left[\int_G (Z - Z_g)^2 d\mu_G(g)\right],$$

because by  $G$ -invariance of  $P$  we may replace  $(g, h)$  by  $(e, g)$  under the expectation/integration (or apply (6) with  $Z$  in place of  $Z_g$ ). This proves (4). The finite-group formulas (5) are the same identities with integrals replaced by uniform averages over  $G$ .

Finally, the strictness statement follows from (3) and the fact that the gap equals  $\mathbb{E}[\text{Var}(Z \mid \sigma(G))]$ , which is zero iff  $Z$  is  $\sigma(G)$ -measurable, i.e.  $G$ -invariant a.s.  $\square$

Therefore, population residual variance reduces for  $G$ -invariant non-conformity scores.

**Proposition 1** (Variance gap upper bound under Lipschitz loss). *Assume that for every  $y \in \mathcal{Y}$ ,  $u \mapsto s(u, y)$  is  $L$ -Lipschitz, and  $\psi_g$  acts by isometries. Then*

$$\text{Var}(s(f(X), Y)) - \text{Var}(\Pi_G[s; f](X, Y)) \leq \frac{L^2}{2} \mathbb{E}\left[\int_G \|f(X) - \psi_g f(\phi_{g^{-1}} X)\|^2 d\mu_G(g)\right].$$

*Proof.* From the orbit identity,

$$\text{Var}(Z) - \text{Var}(\Pi_G[s; f]) = \frac{1}{2} \mathbb{E}\left[\int_G (Z - Z_g)^2 d\mu_G(g)\right].$$

By  $L$ -Lipschitzness and isometry of  $\psi_g$ ,

$$|Z - Z_g| = |s(f(X), Y) - s(\psi_g f(\phi_{g^{-1}} X), Y)| \leq L \|f(X) - \psi_g f(\phi_{g^{-1}} X)\|.$$

Squaring and integrating yields the claim.  $\square$

**Proposition 2** (Jensen-type lower bound under strong convexity). *Assume  $\mathcal{Y}$  is a real normed vector space, the  $G$ -action  $\psi_g$  acts by isometries on  $\mathcal{Y}$ , and for every  $y \in \mathcal{Y}$ , the map  $u \mapsto s(u, y)$  is  $m$ -strongly convex ( $m > 0$ ) w.r.t.  $\|\cdot\|$ . Define the  $G$ -aligned orbit predictor*

$$U_g(X) := \psi_g(f(\phi_{g^{-1}} X)), \quad \bar{f}_G(X) := \int_G U_g(X) d\mu_G(g).$$

Then for all  $(X, Y)$ ,

$$\Pi_G[s; f](X, Y) = \int_G s(U_g(X), Y) d\mu_G(g) \geq s(\bar{f}_G(X), Y) + \frac{m}{2} \int_G \|U_g(X) - \bar{f}_G(X)\|^2 d\mu_G(g).$$

Consequently,

$$\mathbb{E}[\Pi_G[s; f](X, Y) - s(\bar{f}_G(X), Y)] \geq \frac{m}{2} \mathbb{E}\left[\int_G \|U_g(X) - \bar{f}_G(X)\|^2 d\mu_G(g)\right].$$

Moreover, by Cauchy-Schwarz,

$$\mathbb{E}[(\Pi_G[s; f](X, Y) - s(\bar{f}_G(X), Y))^2] \geq \frac{m^2}{4} \mathbb{E}\left[\left(\int_G \|U_g(X) - \bar{f}_G(X)\|^2 d\mu_G(g)\right)^2\right].$$

*Proof.* By  $G$ -invariance of  $s$ , for each  $g$ ,  $s(f(\phi_{g^{-1}}X), \psi_{g^{-1}}Y) = s(\psi_g f(\phi_{g^{-1}}X), Y) = s(U_g(X), Y)$ . Fix  $(X, Y)$  and set  $\varphi(u) := s(u, Y)$ . Strong convexity of  $\varphi$  gives

$$\int_G \varphi(U_g) d\mu_G(g) \geq \varphi\left(\int_G U_g d\mu_G\right) + \frac{m}{2} \int_G \|U_g - \bar{f}_G\|^2 d\mu_G.$$

Taking expectations yields the two displays. The last inequality is Jensen on the square together with the previous bound.  $\square$

## 4 Symmetry-infused CP with equivariantized pre-trained model

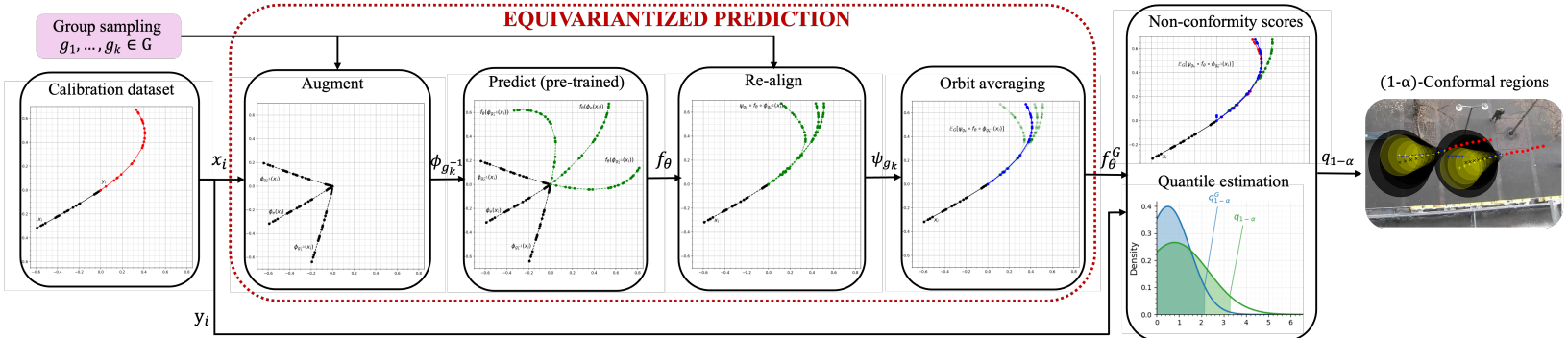


Figure 1: Caption

Consider a pre-trained model  $f_\theta : \mathcal{X} \rightarrow \mathcal{Y}$  on  $\mathcal{D}_{\text{train}}$  and a  $G$ -invariant non-conformity score  $s : (\mathcal{X} \times \mathcal{F}) \times \mathcal{Y} \rightarrow \mathbb{R}_{\geq 0}$  that is, additionally, convex in the prediction argument. Then, one may observe that

$$\begin{aligned} \Pi_G[s; f](x, y) &:= \int_G s(f_\theta(\phi_{g^{-1}}(x)), \psi_{g^{-1}}(y)) d\mu(g) \\ &= \int_G s(\psi_g(f_\theta(\phi_{g^{-1}}(x))), y) d\mu_G(g) \geq s\left(\underbrace{\int_G \psi_g \circ f_\theta \circ \phi_{g^{-1}}(x) d\mu_G(g)}_{f_\theta^G}, y\right) \end{aligned} \quad (7)$$

We now define the equivariantized pre-trained model

$$f_\theta^G(x) := \int_G \psi_g \circ f_\theta \circ \phi_{g^{-1}}(x) d\mu_G(g) = \mathbb{E}_G[\psi_g \circ f_\theta \circ \phi_{g^{-1}}(x)] \quad (8)$$

This is the canonical projection of  $f$  onto the space of  $G$ -equivariant maps. The domain of the non-conformity score is, thus, restricted now to  $s : (\mathcal{X} \times \mathcal{F}_G) \times \mathcal{Y} \rightarrow \mathbb{R}_{\geq 0}$ . The proof that predictor  $f_\theta^G$  is  $G$ -equivariant

is rather similar to that of Lemma 1 and it is obvious that the non-conformity score remain  $G$ -invariant for  $G$ -equivariant models. Furthermore, Theorem 1 still stands, allowing for a more practical implementation of the Equivariantized Split Conformal Prediction. Combining 7 with Lemma 2

$$s\left(\mathbb{E}_G[\psi_g \circ f_\theta \circ \phi_{g^{-1}}(x)], y\right) \leq \mathbb{E}_{(\mathcal{X} \times \mathcal{Y}) \sim P}[s(f_\theta(X), Y) \mid (X, Y) \in \mathcal{O}_{(x, y)}^{(\phi, \psi)}] \quad (9)$$

and taking expectations yields

$$\mathbb{E}_{(\mathcal{X} \times \mathcal{Y}) \sim P}[s(f^G(X), Y)] \leq \mathbb{E}_{(\mathcal{X} \times \mathcal{Y}) \sim P}[s(f(X), Y)] \quad (10)$$

i.e. the non-conformity scores are expected to contract when we equivariantize the pretrained model according to 8. This is owed to the infusion of geometric information at every prediction.

#### 4.1 Risk improvement via increasing convex ordering

**Definition 7** (Increasing convex order). *For integrable random variables  $U, V$ , we write  $U \preceq_{\text{icx}} V$  if  $\mathbb{E}[\phi(U)] \leq \mathbb{E}[\phi(V)]$  for all increasing convex  $\phi : \mathbb{R} \rightarrow \mathbb{R}$ . Equivalently (stop-loss order),*

$$U \preceq_{\text{icx}} V \iff \mathbb{E}[(U - t)_+] \leq \mathbb{E}[(V - t)_+] \quad \forall t \in \mathbb{R}.$$

**Theorem 2** (Orbit symmetrization improves risk in icx ordering). *Consider  $G^{n_c+1} \times \mathbb{S}_{n_c+1}$ -exchangeability and convexity of the  $G$ -invariant non-conformity score  $s$  in its prediction argument. The non-conformity score distributions of the pretrained model and its equivariantized version, then, satisfy*

$$s(f^G(X), Y) = S_{f^G} \preceq_{\text{icx}} S_f = s(f(X), Y), \quad (X, Y) \sim P$$

*Proof.* For  $(X, Y) \sim P$ , from pointwise Jensen's inequality along  $G$ -orbits 7, we have

$$s(f_\theta^G(X), Y) \leq \Pi_G[s; f_\theta](X, Y) \quad \text{a.s.} \quad (11)$$

By Lemma 2, one may identify  $\Pi_G[s; f_\theta]$  as a conditional expectation:

$$\Pi_G[s; f_\theta](X, Y) = \mathbb{E}[s(f_\theta(X), Y) \mid \sigma(G)] = \mathbb{E}[S_f \mid \sigma(G)],$$

where  $\sigma(G)$  is the  $\sigma$ -algebra of  $G$ -invariant events (equivalently, the  $\sigma$ -algebra generated by the orbits). From (11) and the monotonicity of  $\varphi$ :

$$\varphi(S_{f^G}) \leq \varphi(\mathbb{E}[S_f \mid \sigma(G)]) \quad \text{a.s.}$$

By conditional Jensen (convexity of  $\varphi$ ):

$$\varphi(\mathbb{E}[S_f \mid \sigma(G)]) \leq \mathbb{E}[\varphi(S_f) \mid \sigma(G)] \quad \text{a.s.}$$

Taking expectations yields

$$\mathbb{E}[\varphi(S_{f^G})] \leq \mathbb{E}[\varphi(S_f)].$$

Since this holds for every increasing convex  $\varphi$  with finite expectation, we conclude  $S_{f^G} \preceq_{\text{icx}} S_f$ .  $\square$

This means that  $Y$  is "more spread out" than  $X$  in a specific sense, where the "more spread out" property is captured by the behavior of increasing convex functions.

**Remark 1** (Equality cases). *If  $f_\theta$  is already  $G$ -equivariant (so  $f_\theta^G = f_\theta$ ) or if the non-conformity score is affine along the convex hull of the  $G$ -orbit of the predictions (so the Jensen step is tight), then equality holds for all increasing convex  $\varphi$ .*

**Corollary 3** (Moment consequences of increasing convex ordering). *For any  $p \geq 1$  with  $\mathbb{E}[S_f^p] < \infty$ , taking  $\varphi(t) = t^p$  gives  $\mathbb{E}[S_{f^G}^p] \leq \mathbb{E}[S_f^p]$ . In particular,  $\mathbb{E}[S_{f^G}] \leq \mathbb{E}[S_f]$  and  $\mathbb{E}[S_{f^G}^2] \leq \mathbb{E}[S_f^2]$ .*

The convex order implies the equality of means, i.e., if  $X \leq_{cx} Y$ , then  $\mathbb{E}[X] = \mathbb{E}[Y]$ , and so by taking  $\phi(x) = x^2$ , we obtain that if  $X \leq_{cx} Y$ , then  $\text{Var}[X] \leq \text{Var}[Y]$ . Also, in case  $\mathbb{E}[X] = \mathbb{E}[Y]$ , then  $X \leq_{cx} Y \Leftrightarrow X \leq_{icx} Y$ .

**Theorem 3** (CVaR contraction under orbit symmetrization). *Fix  $\alpha \in [0, 1)$  and assume  $\mathbb{E}[S_f^+] < \infty$ . Under the assumptions of Theorem 2, with  $S_f := s(f_\theta(X), Y)$  and  $S_{f^G} := s(f_\theta^G(X), Y)$ ,*

$$\text{CVaR}_\alpha(S_{f^G}) \leq \text{CVaR}_\alpha(S_f).$$

*Proof.* By Theorem 2, we have  $S_{f^G} \preceq_{icx} S_f$ . By the stop-loss characterization of  $\preceq_{icx}$ ,

$$\mathbb{E}[(S_{f^G} - t)_+] \leq \mathbb{E}[(S_f - t)_+] \quad \forall t \in \mathbb{R}. \quad (12)$$

Recall the Rockafellar–Uryasev representation of CVaR for any integrable random variable  $Z$  and  $\alpha \in [0, 1)$ :

$$\text{CVaR}_\alpha(Z) = \inf_{t \in \mathbb{R}} \left\{ t + \frac{1}{1-\alpha} \mathbb{E}[(Z - t)_+] \right\}.$$

Applying this to  $Z = S_{f^G}$  and  $Z = S_f$ , and using (12), we obtain  $\forall t \in \mathbb{R}$ ,

$$t + \frac{1}{1-\alpha} \mathbb{E}[(S_{f^G} - t)_+] \leq t + \frac{1}{1-\alpha} \mathbb{E}[(S_f - t)_+].$$

Taking the infimum over  $t$  on both sides yields

$$\text{CVaR}_\alpha(S_{f^G}) \leq \text{CVaR}_\alpha(S_f).$$

□

## 4.2 Quantile contraction under equivariantization of pre-trained models

**Lemma 3.** *Let  $X$  and  $Y$  be two random variables with cumulative distribution functions  $F$  and  $G$ , and quantile functions  $F^{-1}$  and  $G^{-1}$ , respectively. If  $X \preceq_{icx} Y$ , then:*

$$\int_p^1 F^{-1}(t) dt \leq \int_p^1 G^{-1}(t) dt \quad \text{for all } p \in (0, 1).$$

*Proof.* Recall that for an integrable random variable  $X$ , the *stop-loss transform* is defined by

$$\text{SL}_X(t) := \mathbb{E}(X - t)_+ = \int_t^\infty (1 - F(x)) dx, \quad t \in \mathbb{R}.$$

We will use the following identities, which hold for all such  $X$ :

1. For each  $p \in (0, 1)$ ,

$$\int_p^1 F^{-1}(u) du = \inf_{t \in \mathbb{R}} \{ \text{SL}_X(t) + t(1-p) \}, \quad (13)$$

and the infimum is attained at any  $t$  such that  $F(t) = p$ .

2. Conversely, for each  $t \in \mathbb{R}$ ,

$$\text{SL}_X(t) = \sup_{p \in [0, 1]} \left\{ \int_p^1 F^{-1}(u) du - t(1-p) \right\}. \quad (14)$$

These formulas show that the functions  $t \mapsto \text{SL}_X(t)$  and  $p \mapsto \int_p^1 F^{-1}(u) du$  are Legendre–Fenchel conjugates up to a linear change of variables.

( $\Rightarrow$ ) Assume that  $X \leq_{icx} Y$ . By definition of the increasing convex order, this is equivalent to

$$\text{SL}_X(t) \leq \text{SL}_Y(t), \quad \forall t \in \mathbb{R}.$$

Then, for any  $p \in (0, 1)$ , applying (13) to  $X$  and  $Y$  yields

$$\int_p^1 F^{-1}(u) du = \inf_t \{ \text{SL}_X(t) + t(1-p) \} \leq \inf_t \{ \text{SL}_Y(t) + t(1-p) \} = \int_p^1 G^{-1}(u) du.$$

Hence the stated inequality holds for all  $p$ .

( $\Leftarrow$ ) Conversely, assume that

$$\int_p^1 F^{-1}(u) du \leq \int_p^1 G^{-1}(u) du \quad \forall p \in (0, 1).$$

By (14), for each  $t \in \mathbb{R}$ ,

$$\text{SL}_X(t) = \sup_{p \in [0, 1]} \left\{ \int_p^1 F^{-1}(u) du - t(1-p) \right\} \leq \sup_{p \in [0, 1]} \left\{ \int_p^1 G^{-1}(u) du - t(1-p) \right\} = \text{SL}_Y(t).$$

Thus  $\text{SL}_X(t) \leq \text{SL}_Y(t)$  for all  $t$ , and therefore  $X \leq_{icx} Y$ .

Combining both directions, we have established that

$$X \leq_{icx} Y \iff \int_p^1 F^{-1}(u) du \leq \int_p^1 G^{-1}(u) du \quad \forall p \in (0, 1),$$

which proves the lemma.  $\square$

**Lemma 4.** *Let  $X$  and  $Y$  be two continuous random variables with interval supports and with distribution functions  $F$  and  $G$ , respectively. Let  $h = F^{-1} \circ G$ . Then,  $X \leq_{icx} Y$  implies*

$$\mathbb{E}[\phi(h(Y)) \mid Y > x] \leq \mathbb{E}[\phi(Y) \mid Y > x] \quad \forall x \in \mathbb{R}$$

for any increasing convex function  $\phi$ .

*Proof.* Suppose  $X \leq_{icx} Y$  and  $\phi$  is an increasing convex function. Then, it is well known that  $\phi(X) \leq_{icx} \phi(Y)$ . By Lemma 3, this is equivalent to saying

$$\int_p^1 F_\phi^{-1}(t) dt \leq \int_p^1 G_\phi^{-1}(t) dt \tag{15}$$

$\forall p \in (0, 1)$  and for all increasing and convex  $\phi$ , where  $F_\phi^{-1}(t) = \phi(F^{-1}(t))$  and  $G_\phi^{-1}(t) = \phi(G^{-1}(t))$  are the quantile functions of  $\phi(X)$  and  $\phi(Y)$ , respectively. Evidently, (15) is equivalent to

$$\int_{G(x)}^1 F_\phi^{-1}(t) dt \leq \int_{G(x)}^1 G_\phi^{-1}(t) dt \tag{16}$$

$\forall x \in \mathbb{R}$  and for all increasing convex  $\phi$ . Since

$$\frac{\int_p^1 F^{-1}(t) dt}{1-p} = \mathbb{E}[X \mid X > F^{-1}(p)],$$

(16) is equivalent to

$$\mathbb{E}[\phi(X) \mid \phi(X) > F_\phi^{-1}(G(x))] \leq \mathbb{E}[\phi(Y) \mid \phi(Y) > G_\phi^{-1}(G(x))] \tag{17}$$

Since  $X \stackrel{d}{=} h(Y)$ , where  $h = F^{-1} \circ G$ , (17)  $\Rightarrow \mathbb{E}[\phi(h(Y)) \mid Y > x] \leq \mathbb{E}[\phi(Y) \mid Y > x]$ .  $\square$

**Theorem 4.** Let  $S_f$  and  $S_{f^G}$  be the conformity scores associated with predictors  $f$  and its  $G$ -equivariant symmetrization  $f^G$ , and let  $F_{S_f}^{-1}$  and  $F_{S_{f^G}}^{-1}$  denote their respective quantile functions. Then for  $U \sim \text{Unif}(0, 1)$  it stands that

$$\mathbb{E}\left[F_{S_{f^G}}^{-1}(U)\right] \leq \mathbb{E}\left[F_{S_f}^{-1}(U)\right],$$

*Proof.* From Theorem 2,  $S_{f^G} \preceq_{\text{icx}} S_f$ , meaning that  $\mathbb{E}[\varphi(S_{f^G})] \leq \mathbb{E}[\varphi(S_f)]$  for all increasing convex functions  $\varphi$ . Choosing  $\varphi(t) = t$ , which is increasing and convex, yields

$$\mathbb{E}[S_{f^G}] \leq \mathbb{E}[S_f]. \quad (18)$$

Next, recall the standard identity relating a random variable to its quantile function. If  $X$  has quantile function  $F_X^{-1}$  and  $U \sim \text{Unif}(0, 1)$ , then  $F_X^{-1}(U) \stackrel{d}{=} X$ , and therefore

$$\mathbb{E}[X] = \mathbb{E}[F_X^{-1}(U)] = \int_0^1 F_X^{-1}(u) du. \quad (19)$$

Applying (19) to  $S_{f^G}$  and  $S_f$  and using (18) gives

$$\mathbb{E}\left[F_{S_{f^G}}^{-1}(U)\right] = \mathbb{E}[S_{f^G}] \leq \mathbb{E}[S_f] = \mathbb{E}\left[F_{S_f}^{-1}(U)\right].$$

Equivalently,

$$\int_0^1 F_{S_{f^G}}^{-1}(u) du \leq \int_0^1 F_{S_f}^{-1}(u) du.$$

□

**Theorem 5** (CVaR gap). Let  $S_f$  and  $S_{f^G}$  be the conformity scores associated with predictors  $f$  and its  $G$ -equivariant symmetrization  $f^G$ , and let  $F_{S_f}^{-1}$  and  $F_{S_{f^G}}^{-1}$  denote their respective quantile functions. Then, for the CVaR gap  $\Delta := \text{CVaR}_\alpha(S_f) - \text{CVaR}_\alpha(S_{f^G})$  it stands

$$0 \leq \Delta \leq \frac{\mathbb{E}[S_f - S_{f^G}]}{1 - \alpha}, \quad \forall \alpha \in (0, 1)$$

*Proof.* From Theorem 2,  $S_{f^G} \preceq_{\text{icx}} S_f$ . From CVaR ordering of Theorem 3,  $\text{CVaR}_\alpha(S_{f^G}) \leq \text{CVaR}_\alpha(S_f) \Rightarrow \Delta \geq 0$  and by definition

$$\begin{aligned} \text{CVaR}_\alpha(S_f) - \text{CVaR}_\alpha(S_{f^G}) &= \frac{1}{1 - \alpha} \int_\alpha^1 F_{S_f}^{-1}(u) - F_{S_{f^G}}^{-1}(u) du \\ &= \frac{1}{1 - \alpha} \left[ \int_0^1 F_{S_f}^{-1}(u) - F_{S_{f^G}}^{-1}(u) du - \underbrace{\int_0^\alpha F_{S_f}^{-1}(u) - F_{S_{f^G}}^{-1}(u) du}_{\leq 0 \text{ from } S_{f^G} \preceq_{\text{icx}} S_f} \right] \\ &\leq \frac{1}{1 - \alpha} \left[ \int_0^1 F_{S_f}^{-1}(u) du - \int_0^1 F_{S_{f^G}}^{-1}(u) du \right] = \frac{\mathbb{E}[S_f - S_{f^G}]}{1 - \alpha} \end{aligned}$$

□

### 4.3 Chernoff bound improvement via MGF ordering

Let  $S_f := s(f_\theta(X), Y)$  and  $S_{f^G} := s(f_\theta^G(X), Y)$  denote the nonconformity scores of the baseline and Reynolds-averaged equivariantized predictor, respectively. Define their cumulant generating functions (CGFs)

$$\psi_f(\lambda) = \log \mathbb{E}[e^{\lambda S_f}], \quad \psi_{f^G}(\lambda) = \log \mathbb{E}[e^{\lambda S_{f^G}}].$$

**Lemma 5** (MGF ordering). Under  $G$ -invariance of  $P$  and convexity of  $s(\cdot)$  in the predictor argument,

$$\psi_{f^G}(\lambda) \leq \psi_f(\lambda) \quad \text{for all } \lambda \geq 0.$$

*Proof.* By Jensen's inequality applied to the exponential function and the convexity of  $s$ , we have

$$\mathbb{E}[e^{\lambda s(f_\theta^G(X), Y)}] = \mathbb{E}\left[e^{\lambda s\left(\mathbb{E}_G\left[\psi_g \circ f_\theta \circ \phi_{g^{-1}}(X)\right], Y\right)}\right] \leq \mathbb{E}\left[\mathbb{E}_G[e^{\lambda s(\psi_g \circ f_\theta \circ \phi_{g^{-1}}(X), Y)}]\right] = \mathbb{E}[e^{\lambda s(f_\theta(X), Y)}],$$

using the  $G$ -invariance of  $(X, Y)$ . Taking logs yields the result.  $\square$

Consider the Chernov bound, implied by Markov's inequality:  $\mathbb{B}_{\text{Chernov}}(S_f \geq t) := \inf_{\lambda \geq 0} e^{-\lambda t + \psi_f(\lambda)}$  with  $P(S_f \geq t) \leq \mathbb{B}_{\text{Chernov}}, t \in \mathbb{R}_{\geq 0}$ . Then, via the MGF ordering the following theorem stands.

**Theorem 6** (non-asymptotic Chernoff bound improvement). *For any threshold  $t > 0$ ,*

$$\mathbb{B}_{\text{Chernov}}(S_{f^G} \geq t) := \inf_{\lambda \geq 0} e^{-\lambda t + \psi_{f^G}(\lambda)} \leq \inf_{\lambda \geq 0} e^{-\lambda t + \psi_f(\lambda)} := \mathbb{B}_{\text{Chernov}}(S_f \geq t)$$

Thus, every exponential tail bound (Chernoff, Bernstein, Bennett) for  $S_f$  is uniformly tightened under equivariantization.

#### 4.4 Rate-function dominance and asymptotic consequences

Assume the MGF  $\mathbb{E}[e^{\lambda S_f}]$  is finite in a neighborhood of 0. Define the Legendre transform (the *rate function* theory of Large Deviations)

$$I_{S_f}(t) = \sup_{\lambda \geq 0} \{\lambda t - \psi_f(\lambda)\}, \quad I_{S_{f^G}}(t) = \sup_{\lambda \geq 0} \{\lambda t - \psi_{f^G}(\lambda)\}.$$

Another consequence of the MGF ordering is that the Cramér rate function of the equivariantized model dominates the pre-trained non-symmetric one.

**Lemma 6** (Rate-function dominance). *If  $\psi_{f^G}(\lambda) \leq \psi_f(\lambda)$  for all  $\lambda$ , then  $I_{S_{f^G}}(t) \geq I_{S_f}(t)$  for all  $t$ .*

The ordering  $\psi_{f^G} \leq \psi_f$  means equivariantization suppresses large-deviation mass by averaging over symmetry-related orbits, yielding a steeper rate function and therefore faster tail decay. Geometrically, symmetry alignment redistributes uncertainty within each orbit, producing sharper prediction regions while preserving finite-sample coverage.

**Asymptotic consequence (under standard tightness).** Assume in addition that the Chernoff bound is asymptotically tight on the right tail for  $S_f$  and  $S_{f^G}$  (e.g., Cramér/Bahadur–Rao type conditions so that  $\log \mathbb{P}(S \geq t) \sim -I_S(t)$  as  $t \rightarrow \infty$ ). Then Lemma 6 implies

$$\log \mathbb{P}(S_{f^G} \geq t) \sim -I_{S_{f^G}}(t) \leq -I_{S_f}(t) \sim \log \mathbb{P}(S_f \geq t) \quad (t \rightarrow \infty),$$

i.e.,  $S_{f^G}$  has an *asymptotically lighter* right tail.

**Extreme-quantile contraction (under the same tightness).** Let  $q_{1-\alpha}(S)$  be the  $(1-\alpha)$  right quantile. When  $I_S$  is strictly increasing on the right tail and the above asymptotics hold, the inverse-rate-function approximation gives

$$q_{1-\alpha}(S_f) \approx I_{S_f}^{-1}(\log(1/\alpha)), \quad q_{1-\alpha}(S_{f^G}) \approx I_{S_{f^G}}^{-1}(\log(1/\alpha)),$$

and since  $I_{S_{f^G}} \geq I_{S_f}$  pointwise, we obtain

$$q_{1-\alpha}(S_{f^G}) \leq q_{1-\alpha}(S_f) \quad \text{as } \alpha \rightarrow 0.$$

Hence, at extreme confidence levels, conformal prediction sets built from the equivariantized model have smaller asymptotic radii and expected volumes at fixed coverage.

## 4.5 Tightening Hoeffding's Bound

The preceding sections established that equivariantization reduces both the variance and the moment generating function of the nonconformity scores. We now show that these properties also lead to an improvement in Hoeffding-type concentration, which controls the deviation of empirical averages from their expectations and underpins many finite-sample coverage guarantees in conformal prediction.

Consider  $f_\theta$  model trained on  $D_{\text{train}}$  and  $D_{\text{cal}} = (X_i, Y_i)_{i=1:n_c}$  calibration set, both drawn i.i.d. from a  $G$ -invariant distribution. For  $G$ -invariant and convex  $s : \mathcal{Y} \times \mathcal{Y} \rightarrow \mathbb{R}_{\geq 0}$ , consider  $S_{f,i} = s(f(X_i), Y_i)$  and  $S_{f^G,i} = s(f^G(X_i), Y_i)$  non-conformity scores on  $D_{\text{cal}}$  for the pre-trained model and its equivariantized form. Assume  $S_f \in [0, b] \subset \mathbb{R}_{\geq 0}$  almost surely and define the empirical statistics

$$\bar{S}_{n_c} = \frac{1}{n_c} \sum_{i=1}^{n_c} S_{f,i} \quad , \quad \bar{S}_{n_c}^G = \frac{1}{n_c} \sum_{i=1}^{n_c} S_{f^G,i}$$

Hoeffding's inequality yields

$$P(|\bar{S}_{n_c} - \mathbb{E}[S_f]| > \varepsilon) \leq 2 \exp\left(-\frac{2n_c \varepsilon^2}{b^2}\right) =: \mathbb{B}_{\text{Hoeffding}}(\bar{S}_{n_c}) \quad (20)$$

**Lemma 7.** *Equivariantized predictors 8 yield tighter Hoeffding-type bounds, i.e.  $\mathbb{B}_{\text{Hoeffding}}(\bar{S}_{n_c}) \geq \mathbb{B}_{\text{Hoeffding}}(\bar{S}_{n_c}^G)$*

*Proof.* From Jensen's inequality

$$s(f_\theta^G(X_i), Y_i) \leq \mathbb{E}_g\left[s\left(f_\theta(\phi_{g^{-1}}(X_i)), \psi_{g^{-1}}(Y_i)\right)\right]$$

Because the group actions  $\varphi_g$  and  $\psi_g$  are  $G$ -isometries (measure-preserving transformations) and  $S_f \in [0, b]$

$$0 \leq s\left(f_\theta(\phi_{g^{-1}}(X_i)), \psi_{g^{-1}}(Y_i)\right) \leq b \quad \forall g \in G$$

After averaging over the orbit,  $b_G := \sup_{(X_i, Y_i)} s(f_\theta^G(X_i), Y_i) \leq b$  and  $\mathbb{B}_{\text{Hoeffding}}(\bar{S}_{n_c}) \geq \mathbb{B}_{\text{Hoeffding}}(\bar{S}_{n_c}^G)$ .  $\square$

Equivariantization therefore provides a potentially tighter exponential tail bound whenever the score varies nontrivially across group orbits, as averaging (a projection), so it cannot expand the score range; it preserves or contracts it. A sharper bound follows from Bernstein's inequality, which explicitly depends on the variance:

$$P(\bar{S}_{n_c}^G - \mathbb{E}[S_f] > \varepsilon) \leq \exp\left(-\frac{n_c \varepsilon^2}{2 \text{Var}(S_f) + \frac{2}{3} b_G \varepsilon}\right) \quad (21)$$

Since  $S_{f^G} \preceq_{\text{icx}} S_f$ , from Corollary 3  $\text{Var}(S_{f^G}) \leq \text{Var}(S_f)$  and  $b_G \leq b$ , then  $\mathbb{B}_{\text{Bernstein}}(S_{f^G}) \leq \mathbb{B}_{\text{Bernstein}}(S_f)$ . This guarantees at least as strong concentration of calibration statistics around their expectations, which in turn yields tighter empirical quantile estimates and smaller conformal prediction sets. Furthermore, from Equation 10  $\mathbb{E}[S_{f^G}] \leq \mathbb{E}[S_f]$ , meaning that the empirical equivariantized non-conformity scores concentrate faster around a smaller statistical mean. Variance reduction leads to tightening of Chebysev-Cantelli's concentration inequality

$$P(S_{f^G} - \mathbb{E}[S_{f^G}] > \varepsilon) \leq \frac{\text{Var}(S_{f^G})}{\text{Var}(S_{f^G}) + \varepsilon^2} \quad (22)$$

## 5 Expected Shrinkage of Conformal Sets

Consider  $f_\theta : \mathcal{X} \rightarrow \mathcal{Y}$  trained on  $D_{\text{train}}$  and  $D_{\text{cal}} = \{(X_i, Y_i)\}_{i=1:n_c}$  calibration set drawn from a  $G$ -invariant distribution under exchangeability, and consider positive semi-definite,  $G$ -invariant, convex non-conformity score. From Split Conformal Prediction theory, for a test sample  $(X_{n_c+1}, Y_{n_c+1})$  it stands that

$$P(Y_{n_c+1} \in C_{1-\alpha}^{f_\theta}(X_{n_c+1})) \geq 1 - \alpha$$

for prediction set

$$C_{1-\alpha}^{f_\theta}(X_{n_c+1}) = \{y \in \mathcal{Y} : s(f_\theta(X_{n_c+1}), Y_{n_c+1}) \leq F_{S_{f_\theta}}^{-1}(1 - \alpha)\}$$

where  $F_{S_{f_\theta}}^{-1}(1-\alpha) := \{p \in \mathbb{R} \mid F_{S_{f_\theta}}(x) \geq 1-\alpha\}$  the continuous and differentiable quantile function on the CDF  $F_{S_{f_\theta}}$  from  $\mathcal{D}_{\text{cal}}$ . From theorem 1 on Finite-Sample Validity of Equivariantized Split Conformal Prediction, the same probabilistic bound stands for the equivariantized predictor, but the conformal prediction set becomes

$$C_{1-\alpha}^{f_\theta^G}(X_{n_c+1}) = \{y \in \mathcal{Y} : s(f_\theta^G(X_{n_c+1}), Y_{n_c+1}) \leq F_{S_{f_\theta^G}}^{-1}(1-\alpha)\}$$

In this section we motivate the use of eCP compared to classic CP by showing that the expected volume of the conformal sets shrinks for the same miscoverage rate  $\alpha \in (0, 1)$ , i.e.  $\mathbb{E}[\text{Vol}(C_{1-\alpha}^{f_\theta^G})] \leq \mathbb{E}[\text{Vol}(C_{1-\alpha}^{f_\theta})]$ .

## 5.1 From quantile contraction to volume contraction of conformal set

Assuming that  $s(f(x), y) = \|f(x) - y\|$  with a Euclidean or norm-induced geometry,  $C_{1-\alpha}^{f_\theta}(x)$  is a ball (or convex set) centered at  $f_\theta(x)$  with radius  $F_{S_{f_\theta}}^{-1}(1-\alpha)$  of volume

$$\text{Vol}(C_{1-\alpha}^{f_\theta}) = \kappa F_{S_{f_\theta}}^{-1}(1-\alpha)^d \quad \text{and} \quad \text{Vol}(C_{1-\alpha}^{f_\theta^G}) = \kappa F_{S_{f_\theta^G}}^{-1}(1-\alpha)^d$$

Let  $p \sim U(1-\alpha, 1)$ . From the Mean Value Theorem

$$F_{S_{f_\theta}}^{-1}(p)^d - F_{S_{f_\theta^G}}^{-1}(p)^d = dq(p)^{d-1}(F_{S_{f_\theta}}^{-1}(p) - F_{S_{f_\theta^G}}^{-1}(p))$$

for some quantile  $q(p) \in \left[ \min\{F_{S_{f_\theta}}^{-1}(p), F_{S_{f_\theta^G}}^{-1}(p)\}, \max\{F_{S_{f_\theta}}^{-1}(p), F_{S_{f_\theta^G}}^{-1}(p)\} \right]$  and  $\forall p \in (1-\alpha, 1)$  it stands that

$$q_0 := \min\{F_{S_{f_\theta}}^{-1}(1-\alpha), F_{S_{f_\theta^G}}^{-1}(1-\alpha)\} \leq q(p) \leq \max\{F_{S_{f_\theta}}^{-1}(1), F_{S_{f_\theta^G}}^{-1}(1)\} =: q_1$$

with  $q_0 \geq 0$ . Then, the expected shrinkage of the conformal regions for the upper quantiles is

$$\begin{aligned} D\text{Vol}_{1-\alpha} &:= \mathbb{E}_{p \sim U(1-\alpha, 1)}[\text{Vol}(C_p^{f_\theta}) - \text{Vol}(C_p^{f_\theta^G})] = \kappa \mathbb{E}_{p \sim U(1-\alpha, 1)} \left[ F_{S_{f_\theta}}^{-1}(p)^d - F_{S_{f_\theta^G}}^{-1}(p)^d \right] \\ &= d \kappa \mathbb{E}_{p \sim U(1-\alpha, 1)} \left[ q(p)^{d-1} (F_{S_{f_\theta}}^{-1}(p) - F_{S_{f_\theta^G}}^{-1}(p)) \right] \\ &\Rightarrow d q_0^{d-1} \kappa \mathbb{E}_{p \sim U(1-\alpha, 1)} \left[ F_{S_{f_\theta}}^{-1}(p) - F_{S_{f_\theta^G}}^{-1}(p) \right] \leq D\text{Vol}_{1-\alpha} \leq d q_1^{d-1} \kappa \mathbb{E}_{p \sim U(1-\alpha, 1)} \left[ F_{S_{f_\theta}}^{-1}(p) - F_{S_{f_\theta^G}}^{-1}(p) \right] \end{aligned} \quad (23)$$

Observe that the upper quantiles can be restated as  $\text{CVaR}_\alpha(S_{f_\theta}) = \mathbb{E}_{p \sim U(0, 1)}[F_{S_{f_\theta}}^{-1}(p) \mid p \geq 1-\alpha]$  and  $\text{CVaR}_\alpha(S_{f_\theta^G}) = \mathbb{E}_{p \sim U(0, 1)}[F_{S_{f_\theta^G}}^{-1}(p) \mid p \geq 1-\alpha]$ , and 23 becomes

$$d q_0^{d-1} \kappa [\text{CVaR}_\alpha(S_{f_\theta}) - \text{CVaR}_\alpha(S_{f_\theta^G})] \leq D\text{Vol}_{1-\alpha} \leq d q_1^{d-1} \kappa [\text{CVaR}_\alpha(S_{f_\theta}) - \text{CVaR}_\alpha(S_{f_\theta^G})] \quad (24)$$

Applying Theorem 5 in 24 yields

$$0 \leq \mathbb{E}_{p \sim U(1-\alpha, 1)}[\text{Vol}(C_p^{f_\theta}) - \text{Vol}(C_p^{f_\theta^G})] \leq \frac{d \kappa}{1-\alpha} \max\{S_{f_\theta}, S_{f_\theta^G}\}^{d-1} \mathbb{E}[S_{f_\theta} - S_{f_\theta^G}] \quad , \forall \alpha \in (0, 1) \quad (25)$$

## 6 Experiments

We evaluate Equivariantized Conformal Prediction (eCP) on long-horizon pedestrian trajectory prediction, a domain characterized by strong geometric symmetries and rapidly accumulating uncertainty. The experiments are designed to validate the theoretical results of Section 4, namely that equivariantization contracts the distribution of nonconformity scores and yields tighter conformal prediction sets while preserving finite-sample coverage guarantees—especially at high confidence levels. We conduct experiments on standard pedestrian trajectory prediction benchmarks: ETH-UCY [23], the Stanford Drone Dataset [24] and the SportVU NBA movement dataset. These datasets are widely used to evaluate uncertainty in multi-agent, long-horizon forecasting and exhibit planar rotational symmetries. Following standard protocols, each input

consists of an observed pedestrian trajectory of 8 timesteps, and the task is to predict future positions over a 12-step horizon. Uncertainty is quantified by constructing conformal prediction sets over future trajectories. We evaluate eCP on top of two pretrained trajectory predictors with fundamentally different modeling assumptions: 1) **SocialVAE** [25]: a stochastic latent-variable model for multimodal trajectory prediction, 2) **TUTR** [26]: a transformer-based deterministic trajectory predictor. No retraining or fine-tuning is performed. All symmetry injection is applied strictly *post hoc*, demonstrating the model-agnostic nature of eCP. We consider planar rotation symmetry groups of increasing richness  $\mathcal{G} \in \{C_4, C_8, \text{SO}(2)\}$ . For  $\text{SO}(2)$ , group averaging is approximated via Monte Carlo sampling. The resulting methods are denoted  $\text{EqC}_4$ ,  $\text{EqC}_8$ , and  $\text{EqSO}(2)$ , respectively. We employ split conformal prediction with Euclidean displacement error as the nonconformity score. Calibration is performed on a held-out set drawn under exchangeability assumptions, and all results are averaged over 15 random calibration splits. We report two primary metrics that directly capture the efficiency–validity trade-off predicted by theory: 1) **Calibration Quantile**  $Q_{0.05}$ : the empirical 95% conformal radius (lower is better), 2) **Empirical Coverage** ( $\text{Cov}_{95\%}$ ): the fraction of test trajectories contained in the conformal prediction set (target: 95%).

Table 1 summarizes results on ETH-UCY and SDD. Across all datasets and base predictors, equivariantized conformal prediction consistently reduces the calibration quantile by approximately 28% while maintaining coverage close to the nominal level. Equivariantized predictors achieve substantial reductions in  $Q_{0.05}$ , often exceeding 20–30% relative to standard conformal prediction. This confirms the predicted contraction of high quantiles under increasing convex order and CVaR dominance, as indicated by Figure 2. Despite significantly tighter prediction sets, empirical coverage remains close to the target 95% across all datasets and models, validating the finite-sample guarantees of eCP. Performance improves monotonically with the richness of the symmetry group:  $\text{EqSO}(2)$  typically outperforms  $\text{EqC}_8$ , which in turn outperforms  $\text{EqC}_4$ . This aligns with the interpretation of equivariantization as orbit averaging, where larger groups induce stronger variance and tail contraction. Both SocialVAE and TUTR benefit from equivariantization, demonstrating that eCP applies equally well to stochastic and deterministic predictors.

Figure 3 illustrates representative prediction sets produced by standard CP and eCP. Equivariantized prediction regions are visibly tighter, particularly at long horizons, while still enclosing the ground-truth trajectories. These qualitative results mirror the quantitative improvements observed in Table 1. Notably, the largest gains occur at high confidence levels, precisely where standard conformal prediction becomes overly conservative. This empirically supports the Chernoff bound tightening os, CVaR contraction, and extreme-quantile improvements established in Sections 4.2,4.3,4.4.

	ETH		SDD		HOTEL	
	$Q_{0.05} \downarrow$	$\text{Cov}_{95\%} \uparrow$	$Q_{0.05} \downarrow$	$\text{Cov}_{95\%} \uparrow$	$Q_{0.05} \downarrow$	$\text{Cov}_{95\%} \uparrow$
SocialVAE	$3.47 \pm 0.05$	$94.94 \pm 0.36$	$5.19 \pm 0.43$	$94.76 \pm 1.52$	$3.39 \pm 0.05$	$94.99 \pm 0.34$
$\text{EqC}_4$ SocialVAE	$2.77 \pm 0.07$	$94.91 \pm 0.52$	$4.13 \pm 0.44$	$94.95 \pm 1.89$	$2.67 \pm 0.06$	$94.94 \pm 0.43$
$\text{EqC}_8$ SocialVAE	$2.67 \pm 0.06$	$94.98 \pm 0.41$	$3.93 \pm 0.31$	$94.88 \pm 1.58$	$2.56 \pm 0.06$	$95.04 \pm 0.43$
$\text{EqSO}(2)$ SocialVAE	$2.57 \pm 0.07$	$94.98 \pm 0.47$	$3.87 \pm 0.36$	$94.79 \pm 1.67$	$2.45 \pm 0.04$	$94.98 \pm 0.40$
TUTR	$9.84 \pm 0.42$	$94.09 \pm 5.00$	$125.06 \pm 5.16$	$95.11 \pm 1.47$	$3.00 \pm 0.08$	$94.82 \pm 2.12$
$\text{EqC}_4$ TUTR	$6.67 \pm 1.38$	$95.02 \pm 3.88$	$121.41 \pm 12.17$	$94.94 \pm 1.34$	$2.02 \pm 0.38$	$94.86 \pm 2.92$
$\text{EqC}_8$ TUTR	$6.07 \pm 0.71$	$94.52 \pm 4.01$	$120.41 \pm 13.91$	$94.93 \pm 1.72$	$2.59 \pm 0.37$	$94.47 \pm 2.97$
$\text{EqSO}(2)$ TUTR	$5.35 \pm 0.94$	$94.64 \pm 5.36$	$119.50 \pm 5.12$	$95.14 \pm 1.68$	$2.17 \pm 0.30$	$94.92 \pm 2.31$
UNIV						
ZARA <sub>1</sub>						
SocialVAE	$3.81 \pm 0.05$	$95.03 \pm 0.27$	$3.54 \pm 0.06$	$94.98 \pm 0.42$	$3.61 \pm 0.08$	$94.86 \pm 0.51$
$\text{EqC}_4$ SocialVAE	$2.96 \pm 0.07$	$94.93 \pm 0.54$	$2.77 \pm 0.08$	$94.86 \pm 0.55$	$2.83 \pm 0.07$	$94.91 \pm 0.51$
$\text{EqC}_8$ SocialVAE	$2.84 \pm 0.05$	$94.90 \pm 0.43$	$2.67 \pm 0.06$	$94.93 \pm 0.48$	$2.71 \pm 0.07$	$94.98 \pm 0.55$
$\text{EqSO}(2)$ SocialVAE	$2.78 \pm 0.07$	$94.95 \pm 0.53$	$2.57 \pm 0.06$	$94.88 \pm 0.52$	$2.61 \pm 0.05$	$94.90 \pm 0.43$
TUTR	$3.39 \pm 0.09$	$95.01 \pm 0.70$	$2.67 \pm 0.41$	$95.03 \pm 1.74$	$2.78 \pm 0.13$	$94.74 \pm 0.93$
$\text{EqC}_4$ TUTR	$3.18 \pm 0.09$	$95.03 \pm 0.56$	$2.60 \pm 0.24$	$94.92 \pm 1.46$	$2.75 \pm 0.32$	$94.71 \pm 1.50$
$\text{EqC}_8$ TUTR	$3.08 \pm 0.04$	$94.90 \pm 0.38$	$2.73 \pm 0.16$	$94.83 \pm 1.15$	$2.92 \pm 0.20$	$94.73 \pm 1.23$
$\text{EqSO}(2)$ TUTR	$2.95 \pm 0.05$	$94.89 \pm 0.46$	$2.56 \pm 0.28$	$94.80 \pm 1.63$	$2.59 \pm 0.21$	$94.66 \pm 1.46$

Table 1: Calibration Quantile ( $Q\alpha = 0.05$ ) and Empirical Coverage on the test set ( $\text{Cov}_{95\%}$ ) for 15-split conformal prediction from groups  $\mathcal{G} \in \{\text{SO}(2), \text{C4}, \text{C8}\}$  on ETH-UCY and SDD. Our methods are dubbed  $\text{Eq}_{\{\mathcal{G}\}} f_\theta$ .

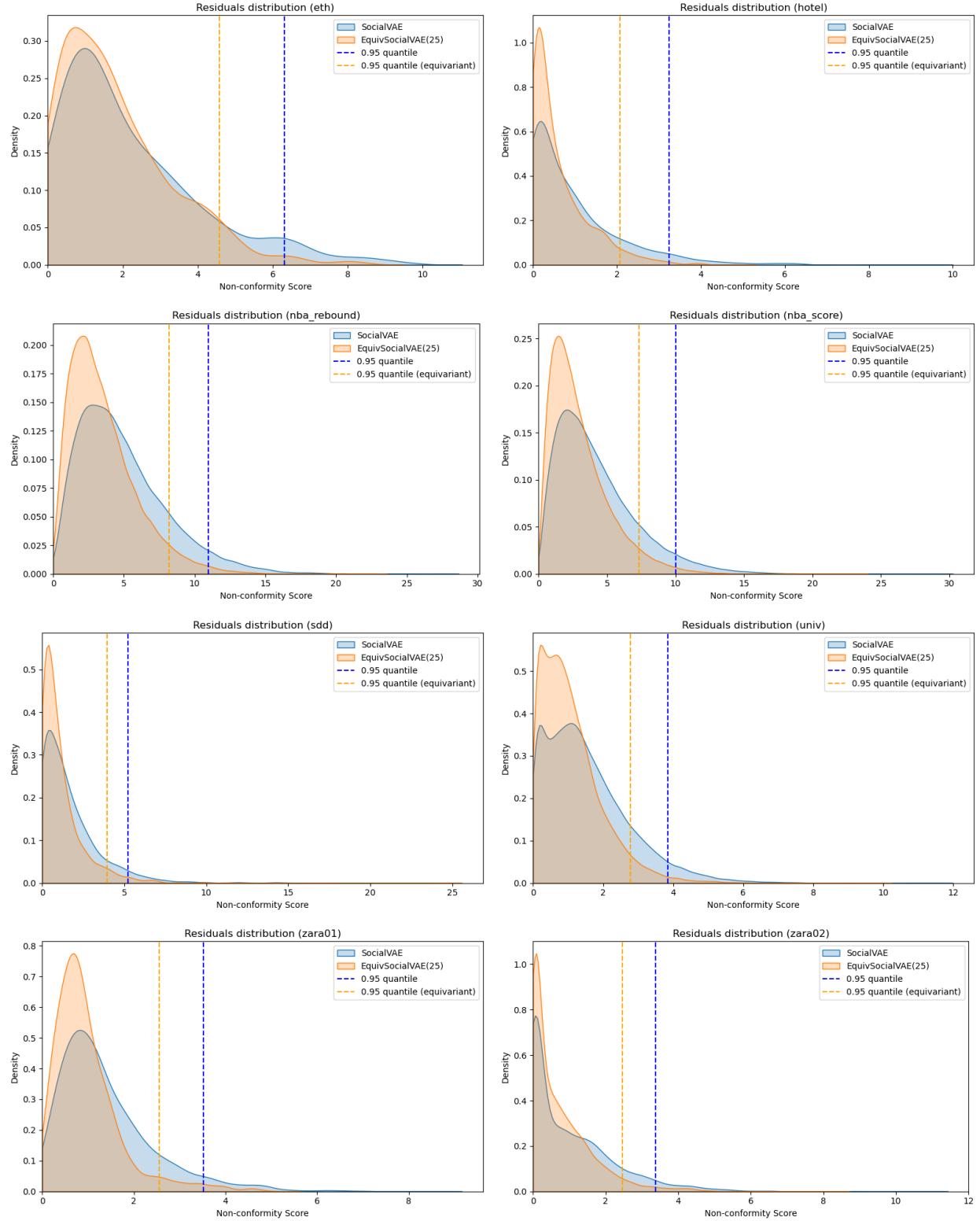


Figure 2: Non-conformity score distributions for SocialVAE and  $\text{EqS}_{\text{SO}_2}\text{SocialVAE}$  with 95<sup>th</sup>-quantile in dashed lines.

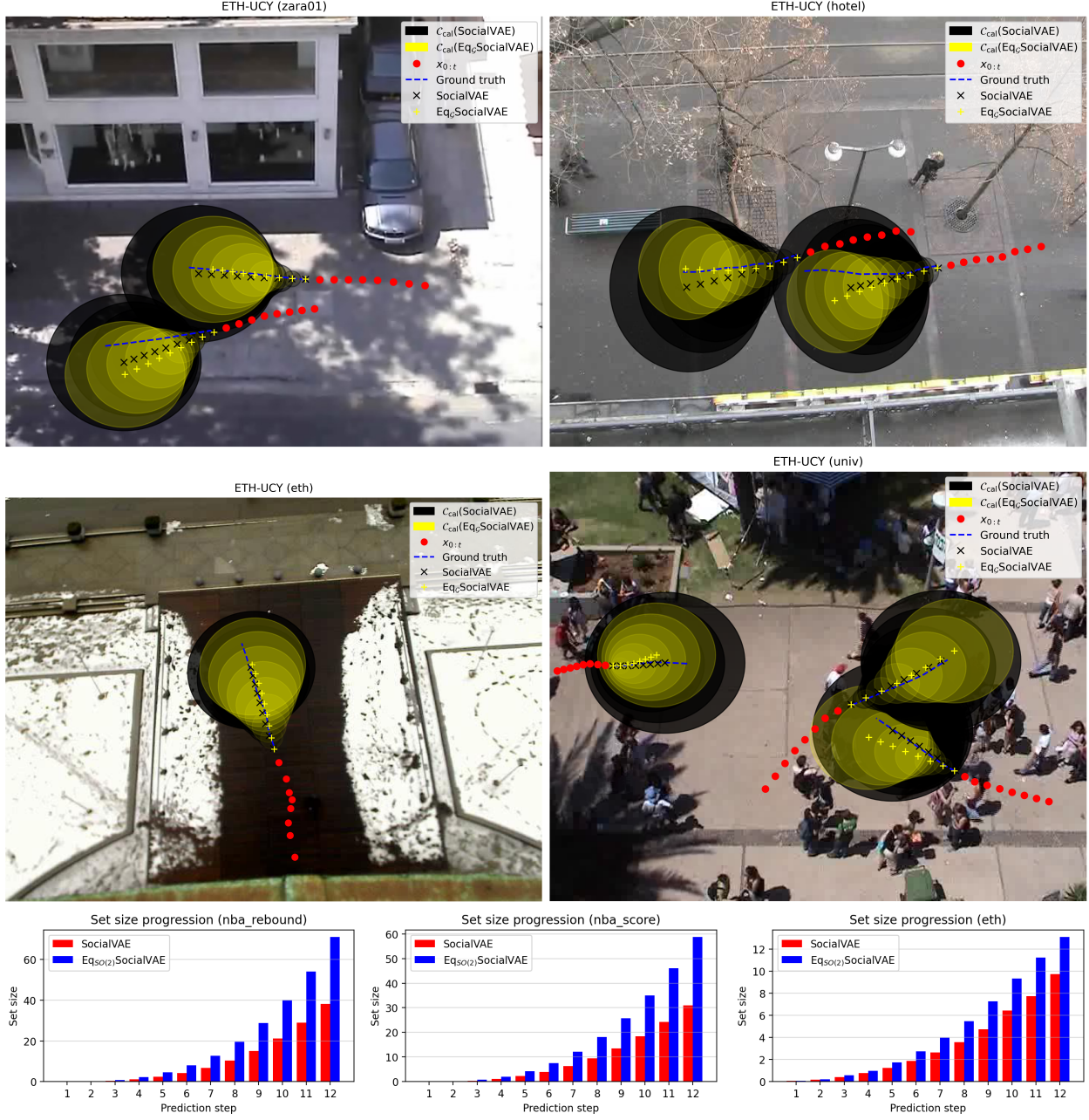


Figure 3: Set size reduction via symmetrization of Conformal prediction in multi-step prediction in ETH-UCY and NBA Rebound/Score datasets.

## 7 Discussion

These results confirm that explicitly injecting symmetry into post-hoc uncertainty quantification yields tangible improvements in efficiency without sacrificing validity. Importantly, eCP requires neither architectural equivariance nor retraining: approximate or emergent symmetry in pretrained models is sufficient to achieve meaningful uncertainty reduction. Overall, the experiments demonstrate that equivariantized conformal prediction provides a principled and practical mechanism for sharpening uncertainty estimates in symmetry-rich, long-horizon forecasting tasks.

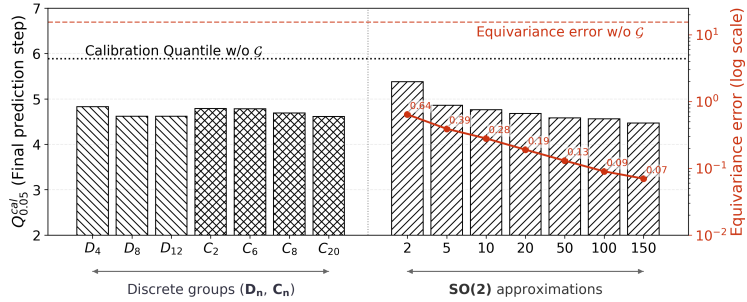


Figure 4: Ablation studies on the group size and approximate equivariance.

	<b>ETH</b>	<b>HOTEL</b>	<b>UNIV</b>	<b>ZARA<sub>1</sub></b>	<b>ZARA<sub>2</sub></b>	<b>NBA Rebound</b>	<b>NBA Score</b>
TUTR	1.83/3.71	0.44/0.90	0.64/1.36	0.43/0.93	0.34/0.75	-	
Eq <sub>C4</sub> TUTR	1.15/2.29	<b>0.34/0.67</b>	0.59/1.26	0.43/0.94	<b>0.32/0.71</b>	-	
Eq <sub>C8</sub> TUTR	1.12/2.26	0.39/0.77	0.55/1.19	0.49/1.09	0.35/0.79	-	
Eq <sub>SO(2)</sub> TUTR	<b>1.08/2.19</b>	<b>0.37/0.73</b>	<b>0.54/1.16</b>	<b>0.49/1.08</b>	0.34/0.77	-	
SocialVAE	0.58/1.28	0.54/1.22	0.64/1.41	0.58/1.30	0.6/1.35	1.86/4.23	2.08/4.91
Eq <sub>C4</sub> SocialVAE	0.46/1.02	0.43/0.96	0.51/1.13	0.47/1.04	0.48/1.06	<b>1.33/3.02</b>	1.50/3.54
Eq <sub>C8</sub> SocialVAE	0.43/0.96	0.41/0.91	0.48/1.06	0.44/0.98	0.45/1.00	<b>1.33/3.01</b>	<b>1.50/3.53</b>
Eq <sub>SO(2)</sub> SocialVAE	<b>0.41/0.92</b>	<b>0.39/0.87</b>	<b>0.47/1.02</b>	<b>0.42/0.94</b>	<b>0.43/0.96</b>	<b>1.33/3.01</b>	<b>1.50/3.53</b>

Table 2: Accuracy comparisons on ETH-UCY and NBA (rebound and scoring) in ADE/FDE.

**Limitations.** While eCP consistently improves the efficiency of conformal prediction sets, several limitations merit discussion. First, the method relies on access to a known or approximately valid symmetry group. If the assumed group poorly reflects the true invariances of the data, equivariantization may yield limited gains. Second, richer symmetry groups incur additional computational cost due to orbit averaging, particularly for continuous groups such as SO(2), which require Monte Carlo approximation. Although this cost is modest relative to model retraining, it may become non-negligible for some real-time systems with strict latency constraints. Finally, our experiments focus on prediction-set tightness and coverage rather than closed-loop planning performance. While tighter uncertainty sets are strongly correlated with improved safety and efficiency in downstream planners, formally quantifying this effect in an integrated planning pipeline remains an important direction for future work.

	ETH		SDD		HOTEL	
	$Q_{0.01} \downarrow$	$\text{Cov}_{99\%} \uparrow$	$Q_{0.01} \downarrow$	$\text{Cov}_{99\%} \uparrow$	$Q_{0.01} \downarrow$	$\text{Cov}_{99\%} \uparrow$
SocialVAE	5.14 $\pm$ 0.19	98.98 $\pm$ 0.21	9.22 $\pm$ 2.60	98.89 $\pm$ 0.60	4.93 $\pm$ 0.26	98.98 $\pm$ 0.29
EqC4SocialVAE	4.26 $\pm$ 0.16	98.97 $\pm$ 0.24	7.08 $\pm$ 1.59	98.93 $\pm$ 0.64	4.10 $\pm$ 0.21	98.97 $\pm$ 0.30
Eq8SocialVAE	4.06 $\pm$ 0.13	98.97 $\pm$ 0.20	6.57 $\pm$ 0.93	98.88 $\pm$ 0.74	3.98 $\pm$ 0.16	98.99 $\pm$ 0.23
EqSO(2)SocialVAE	3.95 $\pm$ 0.14	98.96 $\pm$ 0.20	6.39 $\pm$ 1.46	98.90 $\pm$ 0.77	3.83 $\pm$ 0.12	98.96 $\pm$ 0.20
TUTR	11.51 $\pm$ 3.29	97.88 $\pm$ 2.12	208.32 $\pm$ 61.59	98.81 $\pm$ 1.05	4.72 $\pm$ 0.15	98.98 $\pm$ 0.21
EqC4TUTR	8.05 $\pm$ 0.99	97.66 $\pm$ 2.34	204.23 $\pm$ 88.41	98.89 $\pm$ 0.97	2.88 $\pm$ 0.92	98.68 $\pm$ 1.10
Eq8TUTR	7.40 $\pm$ 1.20	98.08 $\pm$ 1.92	199.65 $\pm$ 47.48	98.81 $\pm$ 0.86	3.55 $\pm$ 0.28	98.88 $\pm$ 1.01
EqSO(2)TUTR	6.31 $\pm$ 0.73	97.80 $\pm$ 2.20	196.27 $\pm$ 33.32	98.85 $\pm$ 0.77	4.21 $\pm$ 0.12	98.95 $\pm$ 0.19
UNIV		ZARA <sub>1</sub>		ZARA <sub>2</sub>		
SocialVAE	5.38 $\pm$ 0.21	98.97 $\pm$ 0.25	5.08 $\pm$ 0.20	98.99 $\pm$ 0.22	5.29 $\pm$ 0.37	98.96 $\pm$ 0.43
EqC4SocialVAE	4.39 $\pm$ 0.22	98.98 $\pm$ 0.30	4.22 $\pm$ 0.20	98.97 $\pm$ 0.27	4.24 $\pm$ 0.14	98.98 $\pm$ 0.20
Eq8SocialVAE	4.22 $\pm$ 0.18	98.99 $\pm$ 0.24	4.07 $\pm$ 0.13	98.98 $\pm$ 0.20	4.11 $\pm$ 0.13	98.98 $\pm$ 0.22
EqSO(2)SocialVAE	4.17 $\pm$ 0.17	98.98 $\pm$ 0.28	3.93 $\pm$ 0.21	98.97 $\pm$ 0.28	3.98 $\pm$ 0.13	98.99 $\pm$ 0.24
TUTR	4.72 $\pm$ 0.15	98.98 $\pm$ 0.21	4.21 $\pm$ 0.66	98.95 $\pm$ 0.71	4.48 $\pm$ 0.31	98.92 $\pm$ 0.43
EqC4TUTR	4.45 $\pm$ 0.12	98.99 $\pm$ 0.20	4.23 $\pm$ 0.44	99.03 $\pm$ 0.74	4.46 $\pm$ 0.41	98.89 $\pm$ 0.64
Eq8TUTR	4.38 $\pm$ 0.27	98.98 $\pm$ 0.35	4.12 $\pm$ 0.34	99.01 $\pm$ 0.59	4.14 $\pm$ 0.24	98.89 $\pm$ 0.57
EqSO(2)TUTR	4.21 $\pm$ 0.12	98.95 $\pm$ 0.19	4.04 $\pm$ 0.25	99.02 $\pm$ 0.53	3.92 $\pm$ 0.15	98.94 $\pm$ 0.29

Table 3: Calibration Quantile ( $Q\alpha = 0.01$ ) and Empirical Coverage on the test set ( $\text{Cov}_{99\%}$ ) for 15-split conformal prediction  $K = 20$  samples from group  $\mathcal{G} \in \{\mathbf{SO}(2), \mathbf{C4}, \mathbf{C8}\}$

## 8 Appendix

**Lemma 8** (Equivariance of Orbit-Averaged Predictor). *The orbit-averaged predictor  $\tilde{f}$  is  $G$ -equivariant:*

$$\tilde{f}(gx) = g \cdot \tilde{f}(x) \quad \text{for all } g \in G, x \in \mathcal{X} \quad (26)$$

*Proof.* By definition:

$$\tilde{f}(gx) = \frac{1}{|G(gx)|} \sum_{h \in G(gx)} h^{-1} f(h(gx)) \quad (27)$$

$$= \frac{1}{|Gx|} \sum_{h \in G} h^{-1} f(hgx) \quad (28)$$

$$= \frac{1}{|Gx|} \sum_{k \in G} (gk)^{-1} f(gkx) \quad (\text{substituting } k = g^{-1}h) \quad (29)$$

$$= \frac{1}{|Gx|} \sum_{k \in G} k^{-1} g^{-1} f(gkx) \quad (30)$$

$$= g \cdot \frac{1}{|Gx|} \sum_{k \in G} k^{-1} f(kx) \quad (31)$$

$$= g \cdot \tilde{f}(x) \quad (32)$$

□

**Lemma 9** (Conditional Mean Domination). *For any orbit  $O = Gx_0$ , if  $s$  is convex in its second argument:*

$$\mathbb{E}[s(X, \tilde{f}(X)) \mid X \in O] \leq \mathbb{E}[s(X, f(X)) \mid X \in O] \quad (33)$$

*Proof.* By  $G$ -invariance of the distribution, the conditional distribution on orbit  $O$  is uniform. Thus:

$$\mathbb{E}[s(X, \tilde{f}(X)) \mid X \in O] = \frac{1}{|O|} \sum_{x \in O} s(x, \tilde{f}(x)) \quad (34)$$

$$= \frac{1}{|O|} \sum_{x \in O} s\left(x, \frac{1}{|O|} \sum_{y \in O} g_{x,y}^{-1} f(y)\right) \quad (35)$$

where  $g_{x,y}$  is the group element such that  $y = g_{x,y}x$ .

By convexity of  $s$  in its second argument:

$$s\left(x, \frac{1}{|O|} \sum_{y \in O} g_{x,y}^{-1} f(y)\right) \leq \frac{1}{|O|} \sum_{y \in O} s(x, g_{x,y}^{-1} f(y)) \quad (36)$$

$$= \frac{1}{|O|} \sum_{y \in O} s(g_{x,y}x, f(y)) \quad (\text{by } G\text{-invariance}) \quad (37)$$

$$= \frac{1}{|O|} \sum_{y \in O} s(y, f(y)) \quad (38)$$

Therefore:

$$\mathbb{E}[s(X, \tilde{f}(X)) \mid X \in O] \leq \frac{1}{|O|} \sum_{x \in O} \frac{1}{|O|} \sum_{y \in O} s(y, f(y)) = \mathbb{E}[s(X, f(X)) \mid X \in O] \quad (39)$$

□

**Lemma 10** (Within-Orbit Variance Elimination). *For any orbit  $O = Gx_0$ , the equivariant predictor  $\tilde{f}$  satisfies:*

$$\text{Var}(s(X, \tilde{f}(X)) \mid X \in O) = 0 \quad (40)$$

*Proof.* By equivariance (Lemma 8), for any  $x, x' \in O$  with  $x' = gx$ :

$$\tilde{f}(x') = \tilde{f}(gx) = g \cdot \tilde{f}(x) \quad (41)$$

By  $G$ -invariance of the non-conformity score:

$$s(x', \tilde{f}(x')) = s(gx, g \cdot \tilde{f}(x)) = s(x, \tilde{f}(x)) \quad (42)$$

Therefore,  $s(x, \tilde{f}(x))$  is constant across the entire orbit  $O$ , implying:

$$\text{Var}(s(X, \tilde{f}(X)) \mid X \in O) = 0 \quad (43)$$

□

## References

- [1] V. Vovk, A. Gammerman, and G. Shafer, *Algorithmic Learning in a Random World*. Springer, 2005.
- [2] G. Shafer and V. Vovk, “A tutorial on conformal prediction,” *Journal of Machine Learning Research*, vol. 9, pp. 371–421, 2008.
- [3] J. Lei, M. G’Sell, A. Rinaldo, R. J. Tibshirani, and L. Wasserman, “Distribution-free predictive inference for regression,” *Journal of the American Statistical Association*, vol. 113, no. 523, pp. 1094–1111, 2018.
- [4] A. N. Angelopoulos and S. Bates, “A gentle introduction to conformal prediction and distribution-free uncertainty quantification,” *Foundations and Trends in Machine Learning*, vol. 16, no. 4, pp. 494–682, 2021.
- [5] Y. Romano, E. Patterson, and E. J. Candès, “Conformalized quantile regression,” in *Advances in Neural Information Processing Systems (NeurIPS)*, 2019.
- [6] R. J. Tibshirani, R. F. Barber, E. J. Candès, and A. Ramdas, “Conformal prediction under covariate shift,” in *Advances in Neural Information Processing Systems*, 2019.
- [7] A. Gibbs and E. J. Candès, “Adaptive conformal inference under distribution shift,” in *Advances in Neural Information Processing Systems*, 2021.
- [8] T. S. Cohen and M. Welling, “Group equivariant convolutional networks,” in *Proceedings of the 33rd International Conference on Machine Learning*, pp. 2990–2999, 2016.
- [9] T. S. Cohen, M. Geiger, J. Köhler, and M. Welling, “Convolutional networks for spherical signals,” in *Proceedings of the 36th International Conference on Machine Learning*, pp. 1321–1330, 2019.
- [10] M. M. Bronstein, J. Bruna, Y. LeCun, A. Szlam, and P. Vandergheynst, “Geometric deep learning: Going beyond euclidean data,” *IEEE Signal Processing Magazine*, vol. 34, no. 4, pp. 18–42, 2017.
- [11] P. A. van der Linden, A. Timans, and E. J. Bekkers, “Cp<sup>2</sup>: Leveraging geometry for conformal prediction via canonicalization,” 2025.
- [12] S. H. Sun and R. Yu, “Copula conformal prediction for multi-step time series prediction,” in *The Twelfth International Conference on Learning Representations*, 2023.
- [13] R. Tumu, M. Cleaveland, R. Mangharam, G. Pappas, and L. Lindemann, “Multi-modal conformal prediction regions by optimizing convex shape templates,” in *Proceedings of the 6th Annual Learning for Dynamics & Control Conference* (A. Abate, M. Cannon, K. Margellos, and A. Papachristodoulou, eds.), vol. 242 of *Proceedings of Machine Learning Research*, pp. 1343–1356, PMLR, 15–17 Jul 2024.

- [14] L. Lindemann, M. Cleaveland, G. Shim, and G. J. Pappas, “Safe planning in dynamic environments using conformal prediction,” *IEEE Robotics and Automation Letters*, vol. 8, no. 8, pp. 5116–5123, 2023.
- [15] J. Sun, Y. Jiang, J. Qiu, P. Nobel, M. J. Kochenderfer, and M. Schwager, “Conformal prediction for uncertainty-aware planning with diffusion dynamics model,” *Advances in Neural Information Processing Systems*, vol. 36, pp. 80324–80337, 2023.
- [16] N. Bousias, S. Pertigkiozoglou, K. Daniilidis, and G. Pappas, “Symmetries-enhanced multi-agent reinforcement learning,” in *Proceedings of the 7th Annual Learning for Dynamics & Control Conference* (N. Ozay, L. Balzano, D. Panagou, and A. Abate, eds.), vol. 283 of *Proceedings of Machine Learning Research*, pp. 999–1011, PMLR, 04–06 Jun 2025.
- [17] N. Bousias, L. Lindemann, and G. Pappas, “Deep equivariant multi-agent control barrier functions,” 2025.
- [18] R. Wang, R. Walters, and R. Yu, “Data augmentation vs. equivariant networks: A theory of generalization on dynamics forecasting,” 2022.
- [19] E. Dobriban and M. Yu, “Symmpi: Predictive inference for data with group symmetries,” 2024.
- [20] J. Pillow and A. Rakhlin, “Predictive inference with group symmetries,” *arXiv preprint arXiv:2203.xxxx*, 2022.
- [21] S. Bates, E. J. Candès, J. Lei, Y. Romano, and R. J. Tibshirani, “Distribution-free predictive inference with exchangeability and invariance,” *Journal of the American Statistical Association*, vol. 118, no. 541, pp. 1–15, 2023.
- [22] A. N. Angelopoulos and S. Bates, “Conformal prediction: A gentle introduction,” *Foundations and Trends in Machine Learning*, vol. 16, no. 5, pp. 494–591, 2023.
- [23] S. Pellegrini, A. Ess, K. Schindler, and L. V. Gool, “You'll never walk alone: Modeling social behavior for multi-target tracking,” in *Proceedings of the IEEE International Conference on Computer Vision*, pp. 261–268, 2009.
- [24] A. Robicquet, A. Sadeghian, A. Alahi, and S. Savarese, “Learning social etiquette: Human trajectory understanding in crowded scenes,” in *Proceedings of the European Conference on Computer Vision*, pp. 549–565, 2016.
- [25] P. Xu, J.-B. Hayet, and I. Karamouzas, “Socialvae: Human trajectory prediction using timewise latents,” in *European Conference on Computer Vision*, pp. 511–528, Springer, 2022.
- [26] H. Zhao, J. Chen, Y. Mao, and Q. Zhang, “Tutr: A transformer-based approach for trajectory prediction,” in *Proceedings of the IEEE/CVF Conference on Computer Vision and Pattern Recognition*, pp. 13133–13142, 2021.